1-1-2014

Isomer Dependence in the Assembly and Lability of Silver(I) Trifluoromethanesulfonate Complexes of the Heteroditopic Ligands, 2-, 3-, and 4-[Di(1*H*-pyrazolyl)methyl]phenyl(di-*p*-tolyl)phosphine

James R. Gardinier
Marquette University, james.gardinier@marquette.edu

Jeewantha S. Hewage
Marquette University, jeewantha.hewage@marquette.edu

Sergey V. Lindeman
Marquette University, sergey.lindeman@marquette.edu

Accepted version. *Inorganic Chemistry,* Vol. 53, No. 22 (2014): 12108-12121. DOI.

Isomer Dependence in the Assembly and Lability of Silver(I) Trifluoromethanesulfonate Complexes of the Heteroditopic Ligands, 2-, 3-, and 4-[Di(1*H*-pyrazolyl)methyl]phenyl(di-*p*-tolyl)phosphine

James R. Gardinier
Department of Chemistry, Marquette University, Milwaukee, WI
Jeewantha S. Hewage
Department of Chemistry, Marquette University, Milwaukee, WI
Sergey V. Lindeman
Department of Chemistry, Marquette University, Milwaukee, WI

Inorganic Chemistry, Vol 53, No. 22 (2014): pg. 12108-12121. DOI.

Synopsis: The solid state and solution structures of silver triflate complexes of the three isomers of new P,N−N heteroditopic ligands are examined.

Abstract

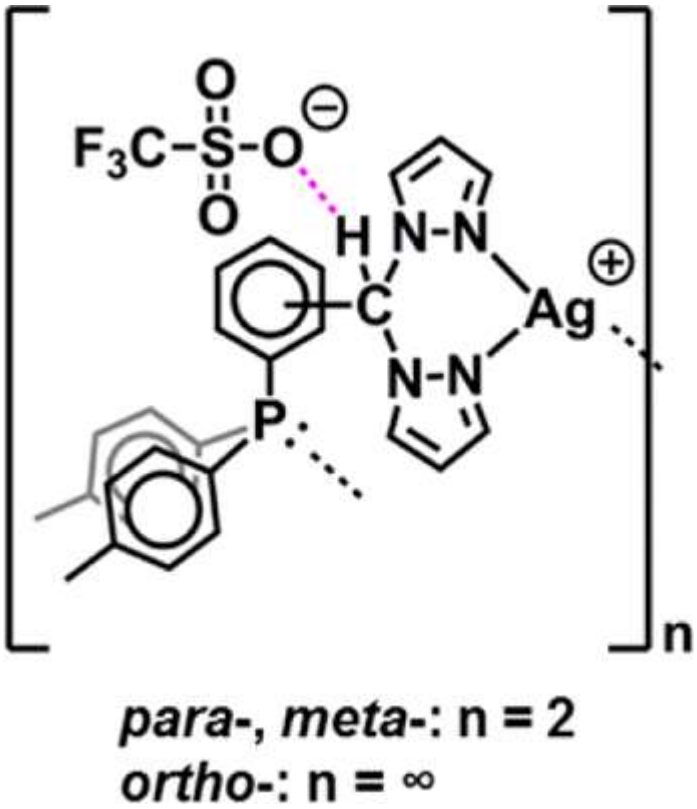

Three isomers of a new heteroditopic ligand that contains a di(1*H*-pyrazolyl)methyl (−$CHpz_2$) moiety connected to a di(*p*-tolyl)phosphine group via a *para*-, *meta*-, or *ortho*-phenylene spacer (***pL***, ***mL***, and ***oL***, respectively) have been synthesized by using a palladium(0)-catalyzed coupling reaction between $HP(p\text{-tolyl})_2$ and the appropriate isomer of $(IC_6H_4)CHpz_2$. The 1:1 complexes of silver(I) trifluoromethanesulfonate, Ag(OTf), were prepared to examine the nature of ligand coordination and the type of supramolecular isomer (monomeric, cyclic oligomeric, or polymeric) that would be obtained. The single crystal X-ray diffraction studies showed that [Ag(***pL***)](OTf), **1**, and [Ag(***mL***)](OTf), **2**, possessed cyclic dimeric dications, whereas [Ag(***oL***)](OTf), **3**, was a coordination polymer. The polymeric chain in **3** could be disrupted by reaction with triphenylphosphine, and the resulting complex, [Ag(***oL***)(PPh_3)](OTf), **4**, possessed a monometallic cation where the ligand was bound to silver in a chelating κ^2*P,N*- coordination mode. The solution structures of **1**–**4** were probed via a combination of IR, variable-temperature multinuclear (^1H, ^{13}C, ^{31}P) NMR spectroscopy, as well as by electron spray ionization (ESI)(+) mass spectrometry. A related complex [Ag(*m*-$IC_6H_4CHpz_2)_2$](OTf), **5**, was also prepared, and its solid-state and solution

Inorganic Chemistry, Vol 53, No. 22 (2014): pg. 12108-12121. DOI.

spectroscopic properties were studied for comparison purposes. These studies suggest that the cyclic structures of **1** and **2** are likely preserved but are dynamic in solution at room temperature. Moreover, both **3** and **4** have dynamic solution structures where **3** is likely extensively dissociated in CH_3CN or acetone rather than being polymeric as in the solid state.

Introduction

There is great interest in the development of coordination polymers because of their myriad possible uses in gas separation and storage,[1] in optical[2] and electronic materials,[3] and even in biological/biomedical[4] applications. Further interest is generated because the ability to modify the organic linker that bridges metal centers offers design opportunities to incorporate new functionality into a coordination polymer[5] or to either probe fundamental or discover new principles of crystal engineering.[6] Multitopic di(pyrazolyl)methane derivatives such as those in Chart 1[7-11] and others[12-16] have proven to be ideal candidates for such studies. Pioneering work by the Reger group on homoditopic α,α,α′α′-tetra(pyrazol-1-yl)-(*p*- or *m*-)xylene ligands, *p*- or *m*-pz_4xyl (Chart 1A, where $n = 0$), showed that the reactions between $AgBF_4$ and the homoditopic ligands in a 1:1 ratio resulted in a coordination polymer with *p*-pz_4xyl but a cyclic bimetallic dication, $[Ag_2L_2]^{2+}$, with *m*-pz_4xyl.[7a] The three-dimensional assembly of the coordination polymer or the derivative with a cyclic dication was governed by ion pairing and directional noncovalent interactions such as the quadruple pyrazolyl embrace,[12d] a concerted set of CH···π and π···π interactions that has been found to be common in structures of metal complexes of poly(pyrazolyl)methane and borate ligands. For other metal complexes of *m*-pz_4xyl, the cyclic bimetallic supramolecular isomer is predominant, persists in solution, and allows for fundamental studies in electronic interactions between two metal centers.[12] Our group recently examined the silver(I) trifluoromethanesulfonate complexes of the six isomers of homoditopic α,α,α′α′-tetra(pyrazol-1-yl)-(X,Y-)dimethylbiphenyl ligands (X,Y = 2, 3, or 4, Chart 1A, $n = 1$, R = H), which showed a similar isomer dependence; cyclic supramolecular isomers were obtained for two of the six possible isomers (2,2- and 3,4-), whereas all other structurally characterized isomers were coordination polymers.[8a] Moreover CH···O interactions between triflate anion and the acidic methine and 5-pyrazolyl hydrogens dominated the

Inorganic Chemistry, Vol 53, No. 22 (2014): pg. 12108-12121. DOI.

supramolecular structures. Concurrently, the Manzano group showed CH···X (X = O, F, Cl, π) noncovalent interactions involving acidic methine, aryl, and pyrazolyl hydrogen and the pyrazolyl embrace govern the solid state assembly of coordination polymers and multimetallic complexes of related biphenyl-linked ligands (Chart1A, *n* = 1, R = Me, 4,4- isomer).[8b] Heteroditopic ligands such as Manzano's (4-py)CHpz*$_2$ (pz* = 3,5-dimethylpyrazol-1-yl, Chart 1B where R = Me),[9] Carrano's (3- or 4-$CO_2HC_6H_4$)CHpz*$_2$ (Chart 1C, R = Me),[10] Marchio's (2-$PhSC_6H_4$)CHpz*$_2$ (Chart 1D),[11] or others[13-16] offer an attractive increase in complexity to the design of solid state architectures because of the different manners in which the ligands could bind metal centers. Thus, Figure 1a–f displays some of the different possible supramolecular isomers of 1:1 M:L complexes of heteroditopic di(pyrazolyl)methane-based ligands that have been observed. The most common structure type is the cyclic bimetallic species in Figure 1d that has different donor ends of two ligands bound to a given metal. Similarly, the most common type of coordination polymer is found in Figure 1a or 1c (the difference being the orientation of the second donor group with respect to the aryl spacer). The complexes [Ag(2-$PhSC_6H_4$)CHpz*$_2$]) (X = BF_4, PF_6, or O_3SCF_3) showed an unusual hexameric metallacyclic structure (Figure 1f). The hexameric rings were inefficiently packed in the solid state by bridging anions and a host of other noncovalent interactions (similar to those shown in the bottom of Figure 1) to give permanent porosity to the crystalline solid and a remarkable capacity and selectivity for CO_2 gas absorption.[11]

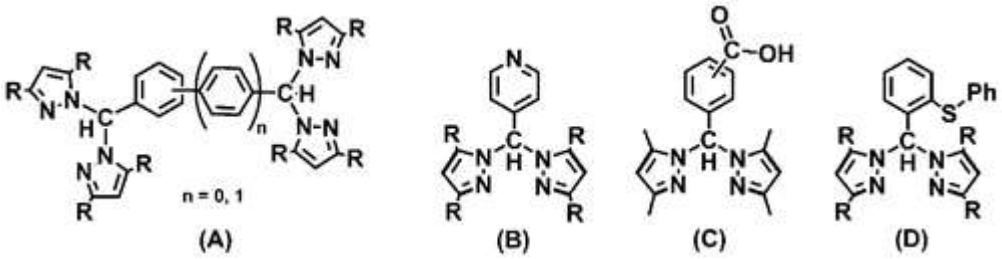

Chart 1. Representative Homo- and Hetero-Ditopic Aryldi(pyrazol-1-yl)methane Ligands (R = H, Me)

Inorganic Chemistry, Vol 53, No. 22 (2014): pg. 12108-12121. DOI.

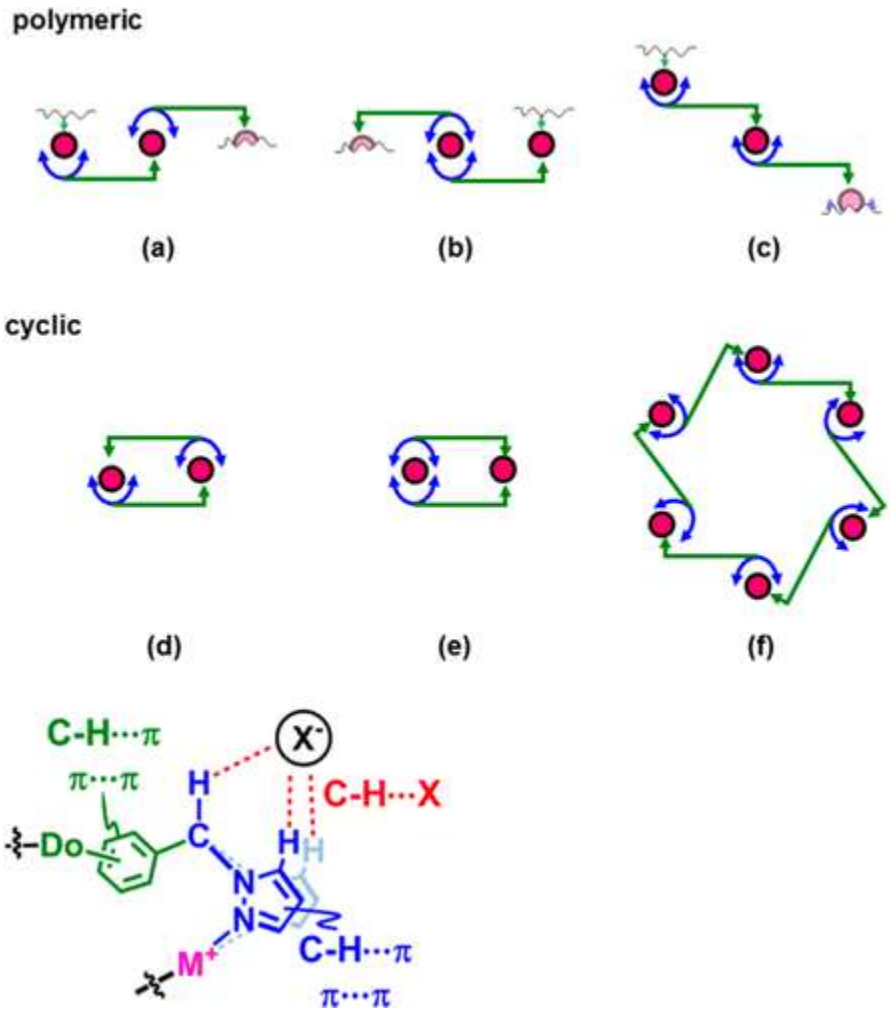

Figure 1. Representative supramolecular isomers of metal complexes of heteroditopic di(pyrazolyl)methane ligands (top and middle) and the common noncovalent interactions that organize their three-dimensional structures (bottom). Key: Di(pyrazolyl)methane unit is blue, the other donor group (Do) and its attached aryl ring is green, and the metal center is pink.

Among the variety of heteroditopic di(pyrazolyl)methane type ligands that have been reported, we were surprised that those with diorganophosphines as a second donor remain unknown. Thus, we set out to prepare $R_2PC_6H_4CHpz_2$ derivatives and explore their coordination chemistry. This contribution outlines our initial endeavors in the preparation of such ligands, specifically, of the three isomers of (*p*-tolyl)$_2$P(C_6H_4)$CHpz_2$. We also detail an investigation into their silver(I) trifluoromethanesulfonate complexes to learn more about the coordination capabilities of the ligands and to examine what effects, if any, a change in disposition of donors around a linking arene ring will

Inorganic Chemistry, Vol 53, No. 22 (2014): pg. 12108-12121. DOI.

have on supramolecular isomers and their three-dimensional crystal packing.

Experimental Section

General Considerations

$Pd(PPh_3)_4$ was prepared according to a literature procedure[17] and stored under argon, and reactions employing this compound were performed under an argon atmosphere. *N*,*N*′-Dimethylethylenediamine (DMED) and all other chemicals were commercially available and were used as received. Solvents were dried by conventional methods and distilled prior to use. Di(*p*-tolyl)phosphine as a 10 wt % solution in hexanes was stored in an argon-filled drybox, and reactions employing this reagent were carried out with the exclusion of air by Schlenk techniques. The syntheses of the silver trifluoromethanesulfonate (AgOTf) complexes were carried out under an argon atmosphere using standard Schlenk techniques and in a foil-covered apparatus to protect AgOTf from light. After complex formation, no special precautions to avoid light or air were taken.

Midwest MicroLab, LLC, Indianapolis, Indiana 45250, performed all elemental analyses. IR spectra were recorded for samples as KBr pellets or as CH_3CN solutions (solution cell with KBr windows) in the 4000–500 cm^{-1} region on a Nicolet Magna-IR 560 spectrometer. ^{1}H, ^{13}C, ^{19}F, and ^{31}P NMR spectra were recorded on a Varian 400 MHz spectrometer. Chemical shifts were referenced to solvent resonances at δ_H 7.26 and δ_C 77.16 for $CDCl_3$, δ_H 2.05 for acetone-d_6, δ_H 1.94 and δ_C 118.26 for CD_3CN or against and external standards of $CFCl_3$ (δ_F 0.00 ppm) or of 85% H_3PO_4 (aq) (δ_P 0.00 ppm). The ^{1}H and ^{13}C NMR data for **1**–**5** are labeled according to Figure S9, Supporting Information and 2D spectra are provided in Figures S10–S13, Supporting Information. Melting point determinations were made on samples contained in glass capillaries using an Electrothermal 9100 apparatus and are uncorrected. Mass spectrometric measurements recorded in ESI(+) mode were obtained on a Micromass Q-TOF spectrometer where formic acid (approximately 0.1% v/v) was added to the mobile phase (CH_3CN).

Inorganic Chemistry, Vol 53, No. 22 (2014): pg. 12108-12121. DOI.

Syntheses

p-$IC_6H_4CH(pz)_2$

A solution of 0.967 g (14.2 mmol) of pyrazole in 10 mL of THF was added to a suspension of 0.341 g (14.2 mmol) of NaH in 10 mL of THF via cannula at a rate slow enough to control hydrogen evolution The flask originally containing pyrazole was washed with an additional 5 mL of THF to ensure quantitative transfer. After hydrogen evolution ceased, a solution of 0.51 mL (1.638 g/mL, 7.1 mmol) of $S(O)Cl_2$ in 10 mL of THF was added to the solution of Na(pz) whereupon a colorless precipitate of NaCl formed. After the suspension of $S(O)pz_2$/NaCl had been stirred 30 min, 0.031 g (0.24 mmol) of $CoCl_2$ was added as a solid in one portion under an argon blanket. After the resulting blue suspension had been stirred 5 min, 1.10 g (4.74 mmol) of 4-iodobenzaldehyde was added under an argon blanket. After the suspension had been heated at reflux or 15 h, it was cooled to room temperature and 100 mL of water was added. The THF fraction was separated from the aqueous. Then the aqueous fraction was extracted with three 50 mL portions ethyl acetate. The combined organic fractions were dried over $MgSO_4$ and filtered, and solvent was removed by rotary evaporation to leave 1.60 g (97%) of *p*-$IC_6H_4CH(pz)_2$ as a white solid. Mp, 100–101 °C. ^{1}H NMR (400 MHz, $CDCl_3$) δ_H 7.70 (d, J = 8.5 Hz, 2 H, Ar), 7.66 (s, 1H, $C_{meth}H$), 7.63 (d, J = 1.5 Hz, 2 H, H_3pz), 7.53 (d, J = 2.3 Hz, 2 H, H_5pz), 6.75 (d, J = 8.5 Hz, 2 H, Ar), 6.35 (pst, J_{app} = 2 Hz, H_4pz) ppm. ^{13}C NMR (100.5 MHz, $CDCl_3$) δ_C 141.1, 138.0, 136.1, 129.9, 128.9, 107.0, 95.6, 77.4 ppm.

The following two compounds were prepared in a similar manner.

m-$IC_6H_4CH(pz)_2$

A mixture of 5.8 mmol of $S(O)pz_2$ [from 0.279 g (11.6 mmol) of NaH, 0.792 g (11.6 mmol) of pyrazole, and 0.42 mL (1.638 g/mL, 5.8 mmol) of $S(O)Cl_2$], 0.025 g (0.19 mmol) $CoCl_2$, and 0.900 g (3.88 mmol) of 3-iodobenzaldehyde gave 0.998 g (73%) of *m*-$IC_6H_4CH(pz)_2$ as a colorless solid after column chromatography (R_f = 0.59, 3:1 hexanes:ethyl acetate, SiO_2) and drying under a vacuum. Mp, 90–91 °C. ^{1}H NMR (400 MHz, $CDCl_3$) δ_H 7.72 (d, J = 7.8 Hz, 1 H, Ar), 7.66

Inorganic Chemistry, Vol 53, No. 22 (2014): pg. 12108-12121. DOI.

(s, 1 H, $C_{meth}H$), 7.64 (d, J = 1.6 Hz, 2 H, H_3pz), 7.54 (d, J = 2.3 Hz, 2 H, H_5pz), 7.36 (s, 1 H, Ar), 7.10 (pst, J_{app} = 7.8 Hz, 1 H, Ar), 6.98 (d, J = 7.8 Hz, 1 H, Ar), 6.36 (pst, J_{app} = 2 Hz, 2 H, H_4pz) ppm. ^{13}C NMR (100.5 MHz, $CDCl_3$) δ_C 141.2, 138.6, 138.5, 136.0, 130.6, 129.9, 126.4, 107.1, 94.7, 76.9 ppm.

o-$IC_6H_4CH(pz)_2$

A mixture of 15.0 mmol of $S(O)pz_2$ [from 0.721 g (30.0 mmol) of NaH, 2.04 g (30.0 mmol) of pyrazole, and 1.09 mL (1.638 g/mL, 15.0 mmol) of $S(O)Cl_2$], 0.130 g (1.00 mmol) of $CoCl_2$, and 2.32 g (10.0 mmol) of 2-iodobenzaldehyde gave a yellow oily mixture after aqueous workup. The organic fraction was passed through a short (50 g) plug of silica gel with the aid of a 3:1 (v:v) ethyl acetate/hexane solution (R_f 0.9) to separate from two pyrazolyl-containing impurities. After solvent was removed, the resulting pale yellow oil crystallized with the aid of scratching the glass to give 3.32 g (95%) of *o*-$IC_6H_4CH(pz)_2$ as a colorless solid. Mp, 81–82 °C. ^{1}H NMR (400 MHz, $CDCl_3$) δ_H 7.90 (dd, J = 7.9, 1.1 Hz, 1 H, Ar), 7.80 (s, 1 H, $C_{meth}H$), 7.66 (dd, J = 1.8, 0.5 Hz, 2 H, H_3pz), 7.35 (td, J = 7.3, 1.2 Hz, 1 H, Ar), 7.32 (d, J = 2.5 Hz, 2 H, H_5pz), 7.09 (td, J = 7.8, 1.6 Hz, 1 H, Ar), 6.73 (dd, J = 7.9, 1.5 Hz, 1 H, Ar), 6.35 (pst, J_{app} = 1.9 Hz, 2 H, H_4pz) ppm. ^{13}C NMR (100.5 MHz, $CDCl_3$) δ_C 141.3, 140.3, 138.2, 131.1, 130.0, 128.8, 128.7, 106.8, 98.3, 81.3 ppm.

p-(*p*-tolyl)$_2$$PC_6H_4CH(pz)_2$, **pL**

A solution of 1.009 g (2.88 mmol) of *p*-$IC_6H_4CH(pz)_2$, 0.10 mL (0.82 g/mL, 1.0 mmol) of DMED, and 20 mL of toluene was purged with argon 15 min and then was transferred via cannula to an argon-purged flask that contained 1.877 g (5.76 mmol) of Cs_2CO_3, 0.017 g (0.0015 mmol) of $Pd(PPh_3)_4$, and 10.0 mL (0.72 g/mL, 10 wt % in hexanes, 3.36 mmol) of HP(*p*-tolyl)$_2$. After the resulting suspension was heated at reflux under argon 15 h, toluene was removed by vacuum distillation to leave a black solid. The black solid was dissolved in a biphasic mixture of 100 mL of H_2O and 50 mL of ethyl acetate. The layers were separated, and the aqueous portion was extracted with two 50 mL portions ethyl acetate. The combined organic fractions were dried over $MgSO_4$ and filtered, and then solvent was removed by

Inorganic Chemistry, Vol 53, No. 22 (2014): pg. 12108-12121. DOI.

vacuum distillation. The resulting oily residue was purified by column chromatography in silica gel. Elution with 4:1 hexanes/ethyl acetate gave 0.987 g (79%) of ***p*L** as a viscous syrup after solvent was removed from the second band (R_f = 0.38). ^{1}H NMR (400 MHz, $CDCl_3$) δ_H 7.72 (s, 1 H, $C_{meth}H$), 7.62 (d, J = 1.3 Hz, 2 H, H_3pz), 7.52 (d, J = 2.2 Hz, 2 H, H_5pz), 7.25 (d, J = 7.5 Hz, 2 H, Ar),7.18 (d, J = 7.6 Hz, 4 H, Ar), 7.13 (d, J = 7.6 Hz, 4 H, Ar), 6.93 (d, J = 7.5 Hz, 2 H, Ar), 6.32 (dd, J = 2, 1 Hz, 2 H, H_4pz), 2.33 (s, 6 H, CH_3) ppm. ^{13}C NMR (100.5 MHz, $CDCl_3$) δ_C 140.8, 140.0 (d, J_{CP} = 12.8 Hz), 139.0, 136.2, 133.9 (d, J_{CP} = 20.1 Hz), 133.6 (d, J_{CP} = 18.9 Hz), 133.1 (d, J_{CP} = 9.0 Hz), 129.8, 129.4 (d, J_{CP} = 7.4 Hz), 126.9 (d, J_{CP} = 6.4 Hz), 106.7, 77.6, 21.3 ppm. ^{31}P NMR (161.8 MHz, $CDCl_3$) δ_P −7.6 ppm.

The following two compounds were prepared similarly.

m-(*p*-tolyl)$_2$PC_6H_4CH(pz)$_2$, ***m*L**

A mixture of 0.931 g (2.86 mmol) of Cs_2CO_3, 5.10 mL (0.72 g/mL, 10 wt % in hexanes, 1.71 mmol) of HP(*p*-tolyl)$_2$, 0.0083 g (7.2 μmol) of $Pd(PPh_3)_4$, 0.500 g (1.43 mmol) of *m*-IC_6H_4CH(pz)$_2$, 0.10 mL (0.82 g/mL, 0.86 mmol) of DMED and 15 mL of toluene gave 0.229 g (37%) ***m*L** as a colorless oil after solvent was removed from the second band obtained from column chromatography (R_f = 0.69, 3:1 hexanes: ethyl acetate, SiO_2). ^{1}H NMR (400 MHz, $CDCl_3$) δ_H 7.65 (s, 1 H, $C_{meth}H$), 7.55 (d, J = 1.3 Hz, 2 H, H_3pz), 7.42 (d, J = 2.4 Hz, 2 H, H_5pz), 7.29 (m, J = 7.6 Hz, 3 H, Ar), 7.10 (br m, 9 H, Ar), 6.91 (d, J = 6.5 Hz, 1 H, Ar), 6.85 (d, J = 7.2 Hz, 1 H, Ar), 6.25 (dd, J = 2, 1 Hz, 2 H, H_4pz), 2.32 (s, 6 H, CH_3) ppm. ^{13}C NMR (100.5 MHz, $CDCl_3$) δ_C 140.8, 139.4 (d, J_{CP} = 13.3 Hz), 139.0, 136.4 (d, J_{CP} = 6.2 Hz), 134.3 (d, J_{CP} = 18.4 Hz), 133.8 (d, J_{CP} = 19.6 Hz), 133.1 (d, J_{CP} = 9.5 Hz), 131.9 (d, J_{CP} = 19.8 Hz), 129.7, 129.5 (d, J_{CP} = 7.3 Hz), 128.8 (d, J_{CP} = 6.3 Hz), 129.9, 106.6, 77.7, 21.4 ppm. ^{31}P NMR (161.8 MHz, $CDCl_3$) δ_P −7.1 ppm.

o-(*p*-tolyl)$_2$PC_6H_4CH(pz)$_2$, ***o*L**

A mixture of 0.972 g (2.98 mmol) of Cs_2CO_3, 5.30 mL (0.72 g/mL, 10 wt % soln in hexanes, 1.79 mmol) of HP(*p*-tolyl)$_2$, 0.0086 g (7.8 μmol) of $Pd(PPh_3)_4$, 0.523 g (1.49 mmol) of *o*-IC_6H_4CH(pz)$_2$, 0.05

mL (0.82 g/mL, 0.48 mmol) of DMED and 15 mL of toluene gave 0.594 g (91%) ***o*L** as a colorless solid after solvent was removed from the second band obtained from column chromatography (R_f = 0.46, 4:1 hexanes: ethyl acetate, SiO_2). Mp, 116–117 °C. ^{1}H NMR (400 MHz, $CDCl_3$) δ_H 8.55 (d, J = 7.6 Hz, 1 H, Ar), 7.49 (d, J = 1.3 Hz, 2 H, H_3pz), 7.36 (t, J = 7.3 Hz, 1 H, Ar), 7.29 (t, J = 7.3 Hz, 1 H, Ar), 7.18 (d, J = 2.4 Hz, 2 H, H_5pz), 7.04 (br m, 10 H, Ar), 6.10 (dd, J = 2, 1 Hz, 2 H, H_4pz), 2.31 (s, 6 H, CH_3) ppm. ^{13}C NMR (100.5 MHz, $CDCl_3$) δ_C 140.9, 140.4 (d, J_{CP} = 23.4 Hz), 138.8, 137.0 (d, J_{CP} = 18.5 Hz), 134.7, 133.9 (d, J_{CP} = 19.9 Hz), 132.0 (d, J_{CP} = 6.9 Hz), 129.9, 129.5 (d, J_{CP} = 3.8 Hz), 129.3 (d, J_{CP} = 7.0 Hz), 127.5 (d, J_{CP} = 4.0 Hz), 106.2, 77.4, 75.5 (d, J_{CP} = 28.0 Hz), 21.4 ppm. ^{31}P NMR (161.8 MHz, $CDCl_3$) δ_P −20.1 ppm.

*[Ag(**pL**)](OTf), **1***

A solution of 0.241 g (0.553 mmol) of ***p*L** in 10 mL of THF was added via cannula to a solution of 0.142 g (0.553 mmol) of AgOTf in 10 mL of THF. The flask originally containing ***p*L** was washed with 5 mL of THF, and the washings were transferred to the reaction mixture to ensure quantitative transfer. After the resulting solution had been stirred 4 h, solvent was removed under a vacuum. The residue was washed with two 5 mL portions Et_2O and was dried under a vacuum to leave 0.328 g (86%) of **1** as a colorless solid. Mp, 258–259 °C dec Anal. Calcd (Found) for $C_{28}H_{25}F_3N_4O_3PSAg$: C, 48.50 (48.47); H, 3.63 (3.72); N, 8.08 (8.08). ^{1}H NMR (400 MHz, CD_3CN) δ_H 8.25 (d, J = 2.5 Hz, 2 H, H_5pz), 8.06 (s, 1 H, $C_{meth}H$), 7.84 (d, J = 1.7 Hz, 2 H, H_3pz), 7.16 (dd, J = 11.5, 8.1 Hz, 2 H, H_2Ar), 7.08 (dd, J = 8, 2 Hz, 4 H, H_3Tol), 7.00 (dd, J = 11.7, 7.0 Hz, 4 H, H_2Tol), 6.64 (d, J = 8.0 Hz, 2 H, H_3Ar), 6.57 (dd, J = 2, 1 Hz, 2 H, H_4pz), 2.31 (s, 6 H, CH_3) ppm. ^{13}C NMR (100.5 MHz, CD_3CN) δ_C 144.5 (C_3 pz), 142.2 (C_4^{tol}), 139.6 (C_4^{Ar}), 135.5 (d, J_{CP} = 18.4 Hz, C_2^{Ar}), 135.0 (C_5 pz), 134.2 (d, J_{CP} = 16.8 Hz, C_2^{tol}), 133.2 (d, J_{CP} = 35.8 Hz, $C_1^{tol\ or\ Ar}$), 130.6 (d, J_{CP} = 10.3 Hz, C_3^{tol}), 128.5 (d, J_{CP} = 36.7 Hz, $C_1^{Ar\ or\ tol}$), 128.0 (d, J_{CP} = 11.3 Hz, C_3^{Ar}), 107.7 (C_4 pz), 75.2 (C_{meth}), 21.4 (CH_3) ppm. ^{19}F NMR (376.1 MHz, CD_3CN, 295 K) δ_F −79.3 (s, 3F) ppm. ^{31}P NMR (161.8 MHz, CD_3CN) δ_P 11.3 (d, J_{109AgP} = 736 Hz, J_{107AgP} = 638 Hz,) ppm. LRMS [ESI(+), *m/z*] (Int.) [assign.]: 1417 (1) $[AgL_3]^+$, 1237 (2) $[Ag_2L_2(OTf)]^+$, 981 (12) $[AgL_2]^+$, 762 (39) $[Ag_2L_3]^{2+}$, 544 (100)

Inorganic Chemistry, Vol 53, No. 22 (2014): pg. 12108-12121. DOI.

$[Ag_2L_2]^{2+}$. Crystals suitable for X-ray diffraction were grown by layering an acetone solution of **1** with hexanes and allowing solvents to slowly diffuse over 20 h.

*[Ag(**mL**)](OTf), **2***

A solution of 0.161 g (0.368 mmol) of ***m*L** in 10 mL of THF was transferred quantitatively (by washing the flask with additional 5 mL of THF and transferring the washings) via cannula to a solution of 0.095 g (0.368 mmol) of AgOTf in 10 mL of THF. A colorless precipitate formed immediately. After the suspension had been stirred 4 h, the insoluble portion was collected by filtration, washed with two 5 mL portions Et_2O, and dried under a vacuum for 2 h to give 0.231 g (91%) of **2** as a colorless solid. Mp, 295–297 °C dec Anal. Calcd (Found) for $C_{28}H_{25}F_3N_4O_3PSAg$: C, 48.50 (48.49); H, 3.63 (3.75); N, 8.08 (7.90). ^{1}H NMR (400 MHz, CD_3CN) δ_H 8.13 (d, J = 2.4 Hz, 2 H, H_5pz), 7.93 (s, 1H, $C_{meth}H$), 7.67 (d, J = 1.4 Hz, 2 H, H_5pz), 7.63 (td, J = 7.9, 2.4 Hz, 1 H, C_5^{Ar}), 7.49 (dd, J = 12.9, 7.4 Hz, 1 H, C_6^{Ar}), 7.25 (d, J = 7.1 Hz,4 H, H_3^{tol}), 6.89 (dd, J = 12.2, 8.0 Hz, 4 H, H_2^{tol}), 6.74 (d, J = 8 Hz, 1 H, H_4^{Ar}), 6.43 (dd, J = 2, 1 Hz, 2 H, H_4pz), 5.61 (d, J = 9.5 Hz, 1 H, C_2^{Ar}), 2.40 (s, 6 H, CH_3) ppm. ^{13}C NMR (100.5 MHz, CD_3CN) δ_C 144.6 (C_5pz), 143.2 (C_4^{tol}), 137.5 (d, J_{CP} = 7.0 Hz, C_3^{Ar}), 135.6 (d, J_{CP} = 25.4 Hz, $C_1^{Ar\ or\ tol}$), 135.0 (d, J_{CP} = 27 Hz C_6^{Ar}), 134.7 (C_5pz), 134.3 (d, J_{CP} = 34.6 Hz, C_2^{tol}), 131.1 (d, J_{CP} = 10.7 Hz, C_2^{Ar}), 130.9 (C_5Ar), 130.5 (C_3^{tol}), 129.6 (C_4^{Ar}), 127.2 (d, J_{CP} = 38.9 Hz, $C_1^{tol\ or\ Ar}$), 107.3 (C_4pz), 75.4 (C_{meth}), 21.3 (CH_3) ppm. ^{19}F NMR (376.1 MHz, CD_3CN, 295 K) δ_F −79.3 (s, 3F) ppm. ^{31}P NMR (161.8 MHz, CD_3CN) δ_P 11.1 (d, J_{109AgP} = 740 Hz; J_{107AgP} = 644 Hz) ppm. LRMS [ESI(+), *m*/*z*] (Int.) [assign.]: 1417 (1) $[AgL_3]^+$, 1237 (3) $[Ag_2L_2(OTf)]^+$, 981 (21) $[AgL_2]^+$, 762 (25) $[Ag_2L_3]^{2+}$, 544 (100) $[Ag_2L_2]^{2+}$. Crystals suitable for X-ray diffraction were grown over the course of 12 h by vapor diffusion of Et_2O into an acetonitrile solution of **2**.

*[Ag(**oL**)](OTf), **3***

A solution of 0.178 g (0.407 mmol) of ***o*L** in 10 mL of THF was transferred quantitatively (by washing the flask with additional 5 mL of THF and transferring the washings) via cannula to a solution of 0.105 g (0.407 mmol) of AgOTf in 10 mL of THF. A colorless precipitate

Inorganic Chemistry, Vol 53, No. 22 (2014): pg. 12108-12121. DOI.

formed immediately. After the suspension had been stirred 4 h, the insoluble portion was collected by filtration, washed with two 5 mL portions Et_2O, and dried under a vacuum for 2 h to give 0.238 g (84%) of **3** as a colorless solid. Mp, 225–227 °C, dec Anal. Calcd (Found) for $C_{28}H_{25}F_3N_4O_3PSAg$: C, 48.50 (48.59); H, 3.63 (3.55); N, 8.08 (7.96). ^{1}H NMR (400 MHz, CD_3CN, 295 K) δ_H 8.35 (d, J = 5.0 Hz, 1 H, $C_{meth}H$), 7.84 (dd, J = 7.8, 4.1 Hz, 1 H, H_3^{Ar}), 7.58 (t, J = 7.6 Hz, 1 H, H_4^{Ar}), 7.44–7.42 (br m, 3 H, H_5Ar and H_5pz), 7.30 (d, J = 2 Hz, 2H, H_3pz) 7.27 (br m, 4 H, H_2^{tol}), 7.26 (br m, 4 H, H_3^{tol}), 6.93 (t, J = 8.3 Hz,1 H, H_6^{Ar}), 6.21 (dd, J = 2, 1 Hz, 2 H, H_4pz), 2.37 (s, 6 H, CH_3) ppm. ^{13}C NMR (100.5 MHz, CD_3CN, 295 K) δ_C 143.4 (C_3pz), 142.2 (C_4^{tol}), 139.4 (d, J_{CP} = 14.1 Hz, C_2^{Ar}), 135.3 (d, J_{CP} = 17.7 Hz, C_2^{tol}), 135.1 (C_5pz), 134.1 (d, J_{CP} = 2.7 Hz, C_6^{Ar}), 132.3 (C_4^{Ar}), 132.1 (d, J_{CP} = 26 Hz, $C_1^{Ar\ or\ tol}$), 131.4 (C_3^{tol}), 131.3 (d, J_{CP} = 4.8 Hz, C_5^{Ar}), 130.6 (d, J_{CP} = 6.0 Hz, C_3^{Ar}), 126.6 (d, J_{CP} = 34.7 Hz, $C_1^{tol\ or\ Ar}$), 107.8 (C_4pz), 75.0 (d, J_{CP} = 20.2 Hz, C_{meth}), 21.4 ppm. ^{19}F NMR (376.1 MHz, CD_3CN, 295 K) δ_F −79.3 (s, 3F) ppm. ^{31}P NMR (161.8 MHz, CD_3CN, 295 K) δ_P −1.1 (br s, LWHM = 245 Hz) ppm; (233 K) δ_P −1.6 (d, J_{109AgP} = 660 Hz; J_{107AgP} = 582 Hz) ppm. LRMS [ESI(+), *m*/*z*, CH_3CN/MeOH] (Int.) [assign.]: 1703 (8) $[Ag_2L_3(OTf)(MeOH)]^+$, 1237 (2) $[Ag_2L_2(OTf)]^+$, 1123 (10) $[Ag_3L_4(OTf)(MeOH)]^{2+}$, 979 (100) $[AgL_2]^+$, 687 (21) $[Ag_3L_2(OTf)(MeOH)]^{2+}$, 584 (25) $[AgL(CH_3CN)]^+$, 543 (5) $[AgL]^+$. Crystals suitable for X-ray diffraction were grown over the course of 12 h by vapor diffusion of Et_2O into an acetonitrile solution of **3**.

*[Ag(**oL**)(PPh_3)](OTf), **4***

Upon addition of 0.0265 g (0.101 mmol) of PPh_3 as a solid to a stirred suspension of 0.0700 g (0.101 mmol) of **3** in 20 mL of CH_2Cl_2, a colorless solution formed. After the solution had been stirred 1 h at room temperature, solvent was removed under a vacuum. The residue was washed with two 5 mL portions hexane and was dried under a vacuum to leave 0.0835 g (87%) **4** as a colorless solid. Mp, 225–226 °C, dec Anal. Calcd (Found) for $C_{46}H_{40}F_3N_4O_3P_2SAg$: C, 57.81 (57.68); H, 4.22 (4.18); N, 5.86 (5.84). ^{1}H NMR (400 MHz, acetone-d_6, 295 K) δ_H 8.75 (br s, 1 H), 8.07 (br d, J = 8 Hz, 1 H), 7.71–7.43 (br m, 20 H), 7.41–7.21 (br m, 9 H), 7.06 (br m, 1 H), 6.24 (br s, 2 H, H_4pz), 2.38 (br s, 6 H, CH_3) ppm. ^{13}C NMR (100.5 MHz, acetone-d_6, 295 K) δ_C not reported because broad resonances and low signal-to-

Inorganic Chemistry, Vol 53, No. 22 (2014): pg. 12108-12121. DOI.

noise gave uninformative spectrum even after reasonable acquisition period of 15 h. ^{19}F NMR (376.1 MHz, acetone-d_6, 295 K) δ_F −79.1 (s, 3F) ppm. ^{31}P NMR (161.8 MHz, acetone-d_6, 295 K) δ_P br s +11.8 (LWHM = 290 Hz, 1 P, PPh_3), br s −2.1 (LWHM = 599 Hz, 1 P, P(*p*-tolyl)$_2$) ppm; (193 K) δ_P 11.6 (dd, $J_{109Ag-P}$ = 558 Hz, $J_{107Ag-P}$ = 484 Hz, J_{P-P} = 108 Hz, 1P, PPh_3), −2.4 (dd, $J_{109Ag-P}$ = 457 Hz, $J_{107Ag-P}$ = 396 Hz, J_{P-P} = 108 Hz, 1P, P(*p*-tolyl)$_2$) ppm. Crystals suitable for X-ray diffraction were grown over the course of 15 h by allowing a layer of hexane to diffuse into a dichloromethane solution of **4**.

[Ag(m-IC$_6$H$_4$CH(pz)$_2$)$_2$](OTf), ***5***

A solution of 0.304 g (0.868 mmol) of *m*-IC$_6$H$_4$CH(pz)$_2$ in 10 mL of THF was transferred quantitatively (by washing the flask with an additional 5 mL of THF and transferring the washings) via cannula to a solution of 0.112 g (0.434 mmol) of AgOTf in 5 mL of THF. A colorless precipitate formed after several hours. After the mixture had been stirred 12 h, the insoluble portion was collected by filtration, washed with two 5 mL portions Et_2O, and dried under a vacuum for 2 h to give 0.356 g (86%) of **5** as a colorless solid. Mp, 220–221 °C dec Anal. Calcd (Found) for $C_{27}H_{22}F_3I_2N_8O_3SAg$: C, 33.88 (33.73); H, 2.32 (2.44); N, 11.71 (11.64). ^{1}H NMR (400 MHz, CD_3CN) δ_H 7.85 (d, *J* = 2.5 Hz, 2 H, H_5pz), 7.82 (s, 1 H, $C_{meth}H$), 7.78 (d, *J* = 7.9 Hz, 1 H, C_6^{Ar}), 7.59 (d, *J* = 1.8 Hz, 2 H, H_3pz), 7.20 (s, 1 H, H_2^{Ar}), 7.16 (t, *J* = 7.9 Hz, 1 H, H_5^{Ar}), 6.88 (d, *J* = 7.9 Hz, 1 H, H_4^{Ar}), 6.42 (dd, *J* = 3, 2 Hz, 2 H, H_4pz) ppm. ^{13}C NMR (100.5 MHz, CD_3CN) δ_C 142.7 (C_3pz), 139.4 (C_6^{Ar}), 139.3 (C_3^{Ar}), 136.6 (C_2^{Ar}), 132.8 (C_5pz), 131.5 (C_5^{Ar}), 127.4 (C_4^{Ar}), 107.5 (C_4pz), 94.6 (C_1^{Ar}), 76.0 (C_{meth}) ppm. LRMS [ESI(+), *m*/*z*] (Int.) [assign.]: 807 (100) $[AgL_2]^+$, 498 (23) [AgL(CH$_3$CN)]+, 351 (50) $[HL]^+$, 283 (92) [L-pz]. Crystals suitable for X-ray diffraction were grown over the course of 12 h by vapor diffusion of Et_2O into an acetonitrile solution of **5**.

Crystallography

X-ray intensity data from a colorless block of **1**·acetone, a colorless prism of **2**·CH$_3$CN, a colorless needle of **3**, a colorless prism of **4**, and a colorless prism of **5** were collected at 100.0(1) K with an Oxford Diffraction Ltd. Supernova diffractometer equipped with a 135

Inorganic Chemistry, Vol 53, No. 22 (2014): pg. 12108-12121. DOI.

mm Atlas CCD detector using Mo(Kα) radiation for **1**·acetone, **2**·CH_3CN, **4**, and **5** but Cu(Kα) for **3**. Raw data frame integration and Lp corrections were performed with CrysAlis Pro (Oxford Diffraction, Ltd.).[18] Final unit cell parameters were determined by least-squares refinement of 34071, 14148, 14020, 22446, and 15970 reflections of **1**·acetone, **2**·CH_3CN, **3**, **4**, and **5**, respectively, with $I > 2\sigma(I)$ for each. Analysis of the data showed negligible crystal decay during collection in each case. Direct methods structure solutions, difference Fourier calculations, and full-matrix least-squares refinements against F^2 were performed with Olex2[19] and SHELXTL.[20] A numerical absorption correction based on Gaussian integration over a multifaceted crystal model were applied to the data for each crystal. All non-hydrogen atoms were refined with anisotropic displacement parameters. Hydrogen atoms were placed in geometrically idealized positions and included as riding atoms. For **3**, the unit cell contains four large void spaces with volumes of approximately 266 A^3 (1064/6487 or 16.4% of total cell volume). The voids are filled with heavily disordered solvent (ca. 1:1 Et_2O/CH_3CN). The solvent mask routine implemented in Olex2 was applied to the data to account for the electron density from these solvents. In the structure of **4**, the pyrazolyl group that is not bound to silver is rotationally disordered over two positions in a 1:1 ratio. The triflate anion is disordered over two positions in an 88:12 ratio. The X-ray crystallographic parameters and further details of data collection and structure refinements are given in Table 1.

Table 1. Crystallographic Data Collection and Structure Refinement for **1**·0.5 acetone, **2**·CH_3CN, **3**, and **5**

compound	**1·0.5 acetone**	**2·CH_3CN**	**3**	**4**	**5**
formula	$C_{59}H_{56}Ag_2F_6N_8O_7P_2S_2$	$C_{60}H_{56}Ag_2F_6N_{10}O_6P_2S_2$	$C_{28}H_{25}AgF_3N_4O_3PS$	$C_{46}H_{40}AgF_3N_4O_3P_2S$	$C_{27}H_{22}AgF_3I_2N_8O_3S$
formula weight	1444.92	1468.95	693.42	955.69	957.26
crystal system	monoclinic	monoclinic	orthorhombic	monoclinic	triclinic
space group	$P2_1/c$	$P2_1/n$	*Pbca*	$P2_1/n$	$P\bar{1}$
temperature [K]	100.0(1)	100.0(1)	100.0(1)	100.0(1)	100.0(1)
a [Å]	22.6768(3)	11.8539(2)	21.8299(3)	9.34515(15)	9.4676(3)
b [Å]	11.79225(13)	15.5905(3)	13.12475(11)	13.8176(3)	11.6230(3)
c [Å]	23.7381(3)	17.6390(4)	22.6416(3)	33.1325(6)	15.5967(4)
α [°]	90.00	90.00	90.00	90.00	70.706(2)
β [°]	99.9683(13)	109.318(2)	90.00	90.3273(15)	86.720(2)
γ [°]	90.00	90.00	90.00	90.00	85.857(2)

Inorganic Chemistry, Vol 53, No. 22 (2014): pg. 12108-12121. DOI.

compound	1·0.5 acetone	2·CH_3CN	3	4	5
V [Å^3]	6251.99(14)	3076.30(11)	6487.09(14)	4278.26(13)	1614.65(8)
Z	4	2	8	4	2
D_{calcd} [g cm^{-3}]	1.535	1.586	1.420	1.484	1.969
λ [Å] (Cu or Mo Kα)	0.7107	0.7107	1.54178	0.7107	0.7107
μ [mm^{-1}]	0.820	0.834	6.497	0.654	2.661
abs correction	numerical	numerical	numerical	numerical	numerical
F(000)	2928	1488	2800.0	1952	920.0
θ range [°]	2.76–29.50	2.27–29.49	3.9–73.6	2.85–29.52	2.78–29.52
reflections collected	72140	31390	33869	48712	36367
independent reflns	15868 (R_{Int} = 0.0326)	7707 (R_{Int} = 0.0343)	6431 (R_{Int} = 0.0473)	10814 (R_{Int} = 0.0324)	8114 (R_{Int} = 0.0371)
$T_{min/max}$	0.727/0.827	0.911/0.940	0.173/0.703	0.904/0.947	0.523/0.723
data/restr/param	15868/0/781	7707/0/400	6431/0/372	10814/107/617	8114/0/406
goodness-of-fit on F^2	1.030	1.033	1.070	1.085	1.073
$R1$[a]/$wR2$[b] [$I > 2\sigma(I)$]	0.0301/0.0665	0.0330/0.0712	0.0331/0.0887	0.0408/0.0916	0.0317/0.0624
$R1$/$wR2$ (all data)	0.0384/0.0707	0.0451/0.0777	0.0378/0.0922	0.0493/0.0958	0.0448/0.0698
largest diff peak/hole/e Å^{-3}	0.59/−0.53	0.53/−0.49	0.70/−0.76	1.24/−0.80	1.48/−1.53

[a]$R1 = \Sigma\|\|F_0| - |F_c\|\|/\Sigma|F_0|$.
[b]$wR2 = [\Sigma w(|F_0| - |F_c|)^2/\Sigma w|F_0|^2]^{1/2}$.

Results and Discussion

Synthesis

Scheme 1 summarizes the preparative routes to the ligands and silver complexes.

Inorganic Chemistry, Vol 53, No. 22 (2014): pg. 12108-12121. DOI.

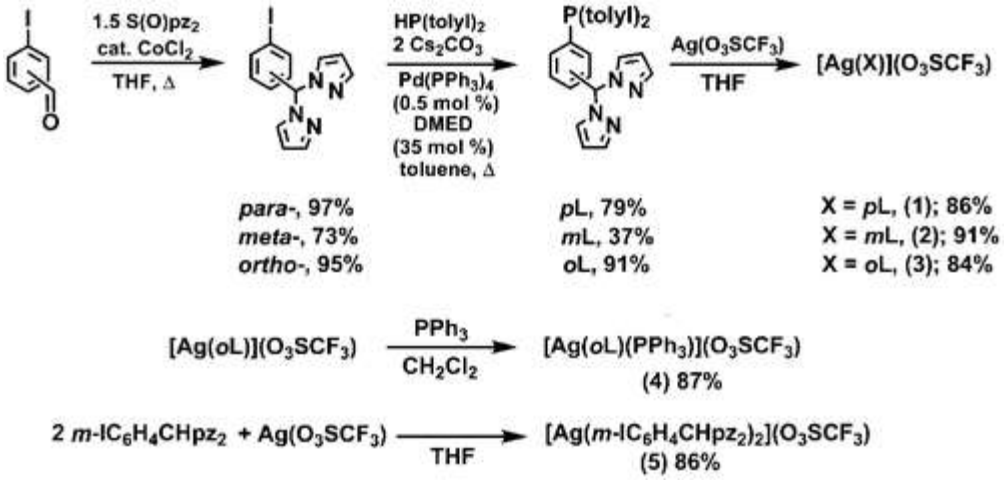

Scheme 1. Preparation of Ligands and Silver Complexes

The di(*p*-tolyl)phosphine group was introduced to the aryldi(pyrazolyl)methane moiety by a palladium(0)-catalyzed coupling reaction between commercial di(*p*-tolyl)phosphine and the easily prepared isomers of $(IC_6H_4)CHpz_2$. The di(*p*-tolyl)phosphine group was chosen over the less expensive diphenylphosphine for the convenience of providing relatively simple ^1H NMR spectral data (vide infra) compared to a diphenylphosphino analogue. This palladium-catalyzed coupling route proceeded smoothly for the *ortho*- and *para*-derivatives. The synthetic yield for the *meta*- derivative was consistently (significantly) lower than that for the other isomers, an observation for which we do not have a satisfactory explanation. Regardless, the current palladium-catalyzed reaction provides a clean route to the ligands. Alternative, perhaps more conventional, routes to the ligands do not proceed as expected. For instance, attempts at lithium aryl exchange between *n*-butyllithium and haloaryldi(pyrazolyl)methane followed by reaction with diarylphosphine halides or esters gave inseparable mixtures due to competitive deprotonation of the acidic methine and (5-)pyrazolyl hydrogens of the $(IC_6H_4)CHpz_2$ moiety. Also, the $CoCl_2$-catalyzed Peterson rearrangement[21] of arylphosphino carboxaldehydes (obtained in low yields) with $S(O)pz_2$ did not give any detectable products perhaps due to poisoning of the metal catalyst by binding to the bulky phosphine. The ensuing reactions between THF solutions of silver(I) trifluoromethanesulfonate, Ag(OTf), and either ***m*L** or ***o*L** in resulted in the immediate precipitation of the desired 1:1 complexes,

Inorganic Chemistry, Vol 53, No. 22 (2014): pg. 12108-12121. DOI.

[Ag(***m*L**)](OTf), **2**, and [Ag(***o*L**)](OTf), **3**. The analogous reaction with ***p*L** did not form a precipitate in THF, as [Ag(***p*L**)](OTf), **1**, is surprisingly more soluble in THF than the other derivatives. All of the complexes are soluble in CH_3CN but are insoluble in Et_2O and hydrocarbon solvents. Complex **1** is significantly more soluble than either **2** or **3** (the latter is nearly insoluble) in CH_2Cl_2. In contrast to **1** and **2**, complex **3** also shows very low solubility acetone. When 1 equiv of triphenylphosphine is added to a suspension of **3** in CH_2Cl_2, a solution is obtained immediately upon mixing since [Ag(***o*L**)(PPh_3)](OTf), **4**, is formed. The complex [Ag(*m*-$IC_6H_4CHpz_2)_2$](OTf), **5**, was isolated in good yield after collecting the precipitate from mixing THF solutions of the ligand and silver salt.

Solid State

Complex **1** crystallized as a hemisolvate, **1**·0.5 acetone, by vapor diffusion of Et_2O into an acetone solution. Views of the structure of **1** are given in Figure 2. The crystal of **1**·0.5 acetone shows a cyclic dimer with two AgN_2PO kernels that arises by the metal coordinating to one oxygen atom of a triflate anion, two pyrazolyl nitrogens from one bridging ligand, and a phosphorus atom from a second bridging ligand (Figure 2a). The average Ag–N_{pz} distance of 2.313 Å is at the lower limit of the 2.3–2.4 Å range previously found for four-coordinate silver bound to pyrazolyl groups.[22] The average Ag–P distance of 2.349 Å is consistent with that found for other silver complexes bound to one phosphine such as (PPh_3)$AgNO_3$ (2.369(6) Å),[23] [(PPh_3)Ag(O_3SCF_3)]$_3$ (avg. 2.345(5),[24a] avg. 2.369(1) Å[24b]), and [(PPh_3)AgCl]$_4$ (2.376(3), 2.388(3) Å).[25] The average Ag–O bond length of 2.49 Å is very close to the average value 2.48(13) Å found for other trifluoromethanesulfonate complexes of silver(I)[26] in a search of the Cambridge Structural Database (CSD),[27] as detailed in the Supporting Information. Analysis of the bond angles about each silver using Hauser's four-coordinate geometry index,[28] $\tau_4 = [360° - (\alpha + \beta)]/141° = 0.67$ for Ag1 and 0.70 for Ag2 where α and β are the largest angles about each silver (138 and 128° for Ag1; 135 and 126° for Ag2), indicates that the coordination geometry is seesaw shaped; a τ_4 value of zero would correspond to a tetrahedron, while a value of 1 would indicate square planar geometry. It is also of interest to note that the dimer formed from two bridging ligands and two silvers is

Inorganic Chemistry, Vol 53, No. 22 (2014): pg. 12108-12121. DOI.

characterized by an 18-member ($Ag_2C_{10}N_4P_2$) metallacycle ring that has a silver–silver separation of 7.65 Å and has approximate local C_2 symmetry of framework (ring) atoms (Figure 2b,c). The conformation of the metallacycle is such that there are two types of *p*-tolyl groups that can be classified as either "axial" (thicker green rings bottom part of Figure 2c) or "equatorial" (thicker violet rings in Figure 2b). The "axial" *p*-tolyl groups are on the same side of the metallacycle ring. Similarly there are two types of pyrazolyl groups, occupying either "axial" or "equatorial" positions with respect to the metallacycle. The "axial" pyrazolyls are found on the same side of the metallacyle ring but on the side opposite of the "axial" *p*-tolyl groups. The 18-member metallacycle deviates from perfect C_2 symmetry as detected by measurement of the AgP–C_{meth}Ag torsion angle, τ_1 (pink lines, Figure 2d), associated with each ligand (τ_1 = 71 and 77°, for ligands A and B, respectively); an acute angle indicates the two silver atoms are on the same side of the central phenylene linker. The τ_1 torsion angle can also be decomposed into two components based on the relative disposition of the silver-bound di(*p*-tolyl)phosphine or di(pyrazolyl)methane unit with respect to the phenyl group that links the moieties. That is, one torsion angle, τ_a (green lines, Figure 2d) defined as the acute angle associated with four atoms AgP–$C_{ipso}C_{ortho}$, essentially describes the rotation of the Ag–P bond from the mean plane of the phenyl linker. A second torsion angle, τ_b (blue lines, Figure 2d) defined as the acute angle of four atoms, AgC_{meth}–$C_{ipso}C_{ortho}$, provides a measure of the rotation of the Ag–C_{meth} vector from coincidence with the mean plane of the phenyl linker (approximated by the C_{ipso}–C_{ortho} bond). Negative values for τ_a and τ_b indicate a clockwise rotation of the Ag–P or Ag–C_{meth} vector from the plane of the phenylene linker (again, approximated by the C_{ipso}–C_{ortho} bond); positive values describe a counter-clockwise rotation. The τ_1, τ_a, and τ_b values for one ligand ("A", containing P1) are 71.1, −12.0, and 80.6°, respectively, whereas those values for the other ligand ("B", containing P2) are 77.2, −41.7, and −67.4°. The different τ_a (or τ_b) values found for ligands A and B of the metallacycle are sufficient to exclude any symmetry relation between ligands.

Inorganic Chemistry, Vol 53, No. 22 (2014): pg. 12108-12121. DOI.

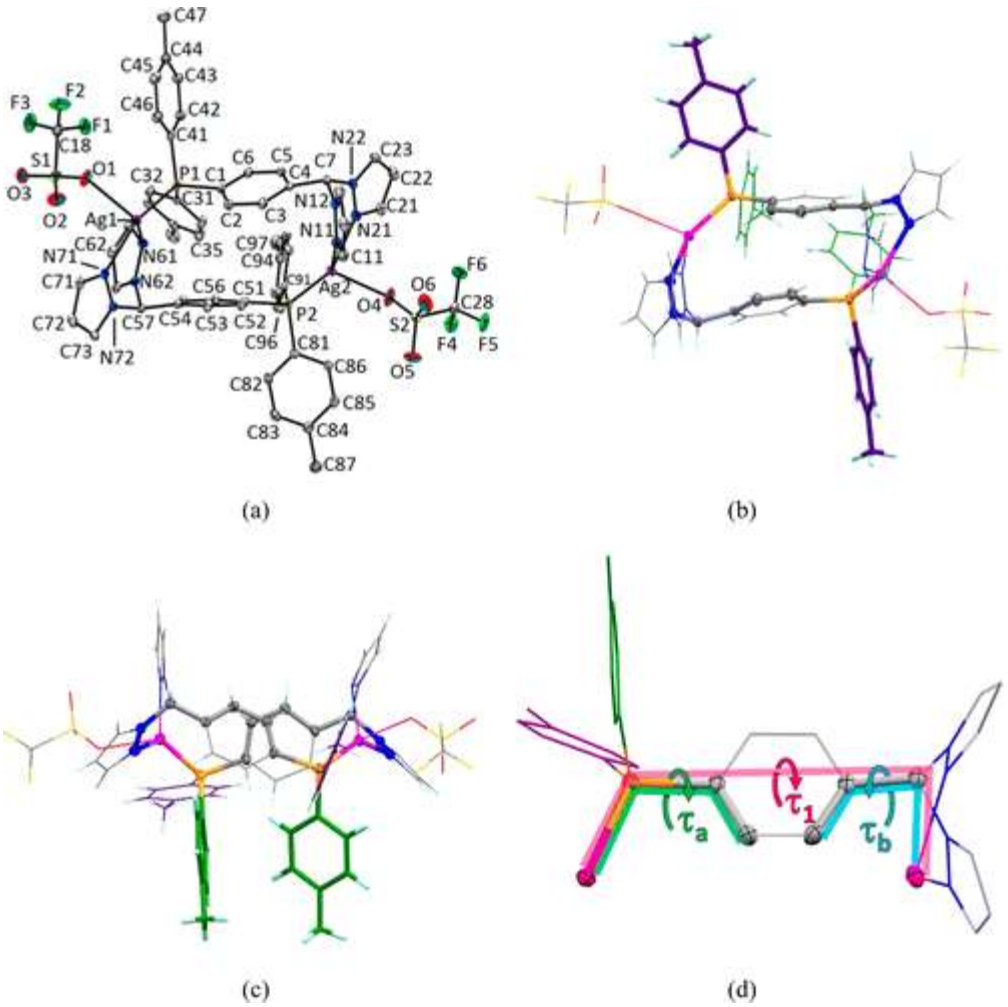

Figure 2. Views of the structure of **1**·0.5 acetone with solvent removed for clarity. (a) Approximately down the *b*-axis; (b) 18-member metallacycle, approximately down the C_2 axis, with equatorial tolyl groups highlighted (violet capped sticks); (c) orthogonal to approximate C_2 axis with axial tolyl groups highlighted (green capped sticks). (d) Labeling scheme of various torsion angles. Selected bond distances (Å): Ag1–P1 2.3555(5), Ag1–O1 2.5125(14), Ag1–N61 2.3336(15), Ag1–N71 2.3094(15), Ag2–P2 2.3445(5), Ag2–O4 2.4734(16), Ag2–N11 2.2713(15), Ag2–N21 2.3361(16). Selected bond angles (°): P1–Ag1–O1 108.27(4), N61–Ag1–P1 127.90(4), N61–Ag1–O1 92.17(5), N71–Ag1–P1 137.84(4), N71–Ag1–O1 97.21(5), N71–Ag1–N61 82.54(5), P2–Ag2–O4 110.51(5), N11–Ag2–P2 135.10(4), N11–Ag2–O4 105.59(6), N11–Ag2–N21 82.67(5), N21–Ag2–P2 126.11(4), N21–Ag2–O4 84.20(6).

Complex **2** crystallizes as a CH_3CN solvate, **2**·CH_3CN, after vapor diffusion of Et_2O into an acetonitrile solution. In this case, a cyclic dimeric dication is formed from two ligands bridging two silver centers with an Ag···Ag separation of 6.003 Å (Figure 3a); the triflate anions are not bound to silver centers[29] as was the previous case. The dication has inversion (C_i point group) symmetry, and thus each silver

Inorganic Chemistry, Vol 53, No. 22 (2014): pg. 12108-12121. DOI.

has an identical planar "Y-shaped" AgN_2P coordination environment (sum of angles about Ag = 360°). The average Ag–N_{pz} bond distance of 2.28 Å is at the upper limit of the 2.2–2.3 Å range found for tricoordinate silver (bound to pyrazolyl donors),[22] and the Ag–P bond distance of 2.3445(6) is nearly identical to the average distance found for **1**·0.5 acetone, which demonstrates previous observations that the Ag–P distance depends mainly on the number of phosphines bound to silver and to a lesser extent on the coordination number of silver.[30] The dication also possesses a 16-member $Ag_2C_8N_4P_2$ metallacylic ring. There are two types of pyrazolyl groups, "axial" and "equatorial", where "axial" pyrazolyls project further above and below the mean plane of the 16-member metallacycle ring than the "equatorial" pyrazolyls, right of Figure 3b. The ring can be said to be in a chair conformation where either "equatorial" or "axial" pyrazolyl nitrogens serve as the "head" and "foot" of the chair. There are also two types of *p*-tolyl groups, "axial" (green, Figure 3b) and "equatorial" (violet, Figure 3b), but the "axial" *p*-tolyl groups are on opposite faces of the mean plane of the metallacycle. Finally, as a means of comparison with **1**, the τ_1, τ_a, and τ_b values for each ligand of the dication in **2** are −25.2, +51.7, +79.4 for one ligand and +25.2, −51.7, −79.4 for the other. The acute τ_1 values in **2** indicate that the two silvers are on the same side of the central phenylene linker, while the identical magnitudes but opposite signs of the τ_1, τ_a, and τ_b values indicate symmetry equivalence (by inversion) of the two ligands.

Inorganic Chemistry, Vol 53, No. 22 (2014): pg. 12108-12121. DOI.

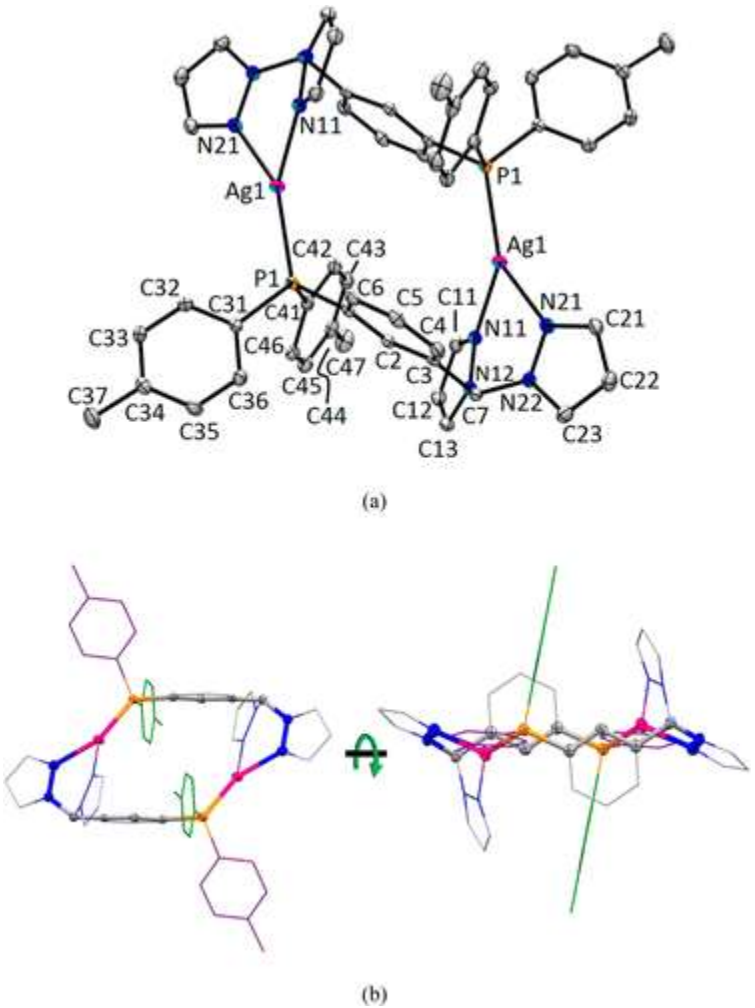

Figure 3. Structure of **2**·CH_3CN. (a) A dimeric dication with atom labeling. Hydrogen atoms, triflate anion and acetonitrile solvate molecule removed for clarity. (b) Views emphasizing 16-member metallacyclic ring and symmetrically distinct *p*-tolyl groups (green and violet).Selected bond distances (Å): Ag1–P1 2.3445(6), Ag1–N11 2.2564(18), Ag1–N21 2.3043(19). Selected bond angles (°): N11–Ag1–P1–144.04(5), N11–Ag1–N21 82.90(7), N21–Ag1–P1 132.63(5).

Complex **3** crystallizes in the orthorhombic space group *Pbca* after vapor diffusion of Et_2O into an acetonitrile solution. The asymmetric unit consists of one ligand, one silver, and one triflate anion, Figure 4a. The ligand again acts in a bridging manner by binding one silver center with the phosphorus atom and another silver with two nitrogens of the $CHpz_2$ moiety. In contrast to the previous cases, the obtuse τ_1 torsion angle of 151.5° in **3** indicates that the silver centers are on opposite faces of the phenylene group that separates the phosphino and di(pyrazolyl)methane groups. This disposition of donor groups results in a coordination polymer instead of

Inorganic Chemistry, Vol 53, No. 22 (2014): pg. 12108-12121. DOI.

a cyclic species, Figure 4b. The coordination polymer propagates along the *b*-direction. Specifically, the polymer is generated by translation of the asymmetric unit along the *b*-glide plane perpendicular to the *a*-axis (i.e., with reflection through the *ac*-plane). The silver centers can be considered either three- or four-coordinate depending on one's view of the long Ag1–O1 contact of 2.809(3) Å, Figure 4c. We favor tetracoordination because this distance is 0.43 Å less than the sum of the van der Waals radii (3.24 Å) and is within 3σ of the average Ag–O distance of 2.48(13) Å found from the CSD (Figure S2, Supporting Information), and since the average Ag–N_{pz} distance of 2.33 Å is in the 2.3–2.4 Å range found for other tetracoordinate silver complexes with pyrazolyl-ligands.[22] If the silver is considered tetracoordinate, then the four-coordinate geometry index, t_4 = 0.60, indicates a seesaw geometry. There are two other contacts, Ag1–O2 3.055(2) Å and Ag1–H7 2.82, that are about 0.2 Å less than the sum of the respective van der Waals radii and, as such, can be considered secondary interactions.

Inorganic Chemistry, Vol 53, No. 22 (2014): pg. 12108-12121. DOI.

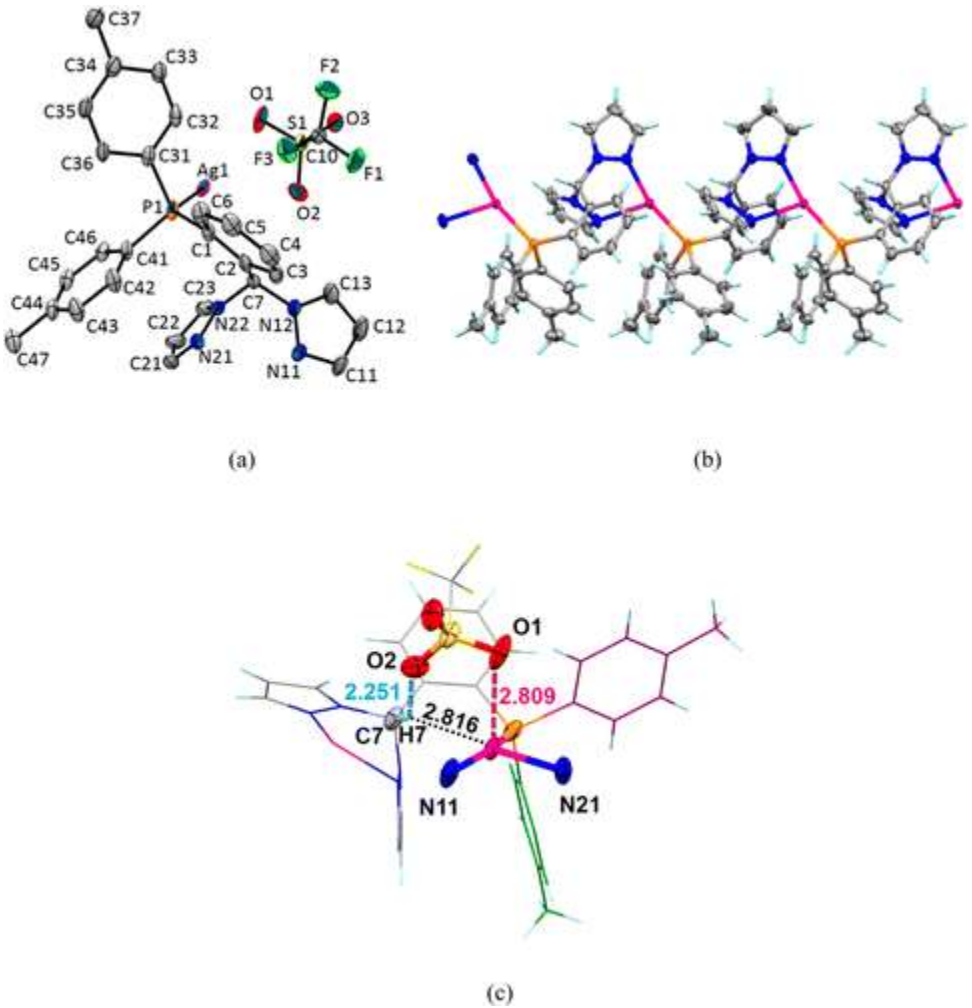

Figure 4. Structure of [Ag(*o*L)](OTf), **3**. (a) Asymmetric unit with atom labeling and with hydrogen atoms removed for clarity. (b) View down the *a*-axis of a chain propagating along the *b*-direction, triflate anions removed for clarity. (c) View of primary and secondary coordination sphere around silver with interatomic distances in Å. Selected bond distances (Å): Ag1–P1 2.3839(6), Ag1–N11 2.266(2), Ag1–N21 2.394(2), Ag1–O1 2.809(3). Selected bond angles (°): P1–Ag1–N21 113.53(6), N11–Ag1–P1 160.73(7), N11–Ag1–N21 83.37(8), P1–Ag1–O1 99.67(5), N11a–Ag1–O1 89.85(9), N21a–Ag1–O1 87.57(8).

The structure of **4** (Figure 5) consists of a monomeric species that has tetracoordinate silver bound to a triphenylphosphine, to ***o*L** in a chelating κ^2*N,P*- manner, and to an oxygen of the triflate anion (in a κ^1- fashion). The structure is afflicted by disorder that allows limited discussion of the coordination environment but precludes extensive analysis of the supramolecular structure. That is, the pyrazolyl ring that is not bound to the silver is rotationally disordered about the C7–N22(a) bond equivalently over two positions. The triflate anion is

located in two nearby positions in an 88:12 ratio, favoring the position depicted on the left of Figure 5 with two oxygen atoms of the anion oriented toward the triphenylphosphine group. The Ag–O distance of either disorder component (Ag1–O1 2.461(3), Ag1–O1a 2.323(17) Å) is shorter than the 2.48 Å average Ag–O(triflate) distance from the above CSD database search, which permits a confident assertion of κ^1*O*- coordination. The Ag–N_{pz} distance of 2.408(2) Å is in line with tetracoordinate silver. The Ag1–P1 distance of 2.5060(6) Å is longer than those distances in **1**–**3** but is consistent with four-coordinate silver complexes of P(*p*-tolyl)$_3$.[31] The Ag–P2 (PPh_3) distance of 2.4186(6) Å is in line with the ca. 2.42 Å average Ag–P distance found in other tetracoordinate silver complexes with two triarylphosphine ligands.[30,32]

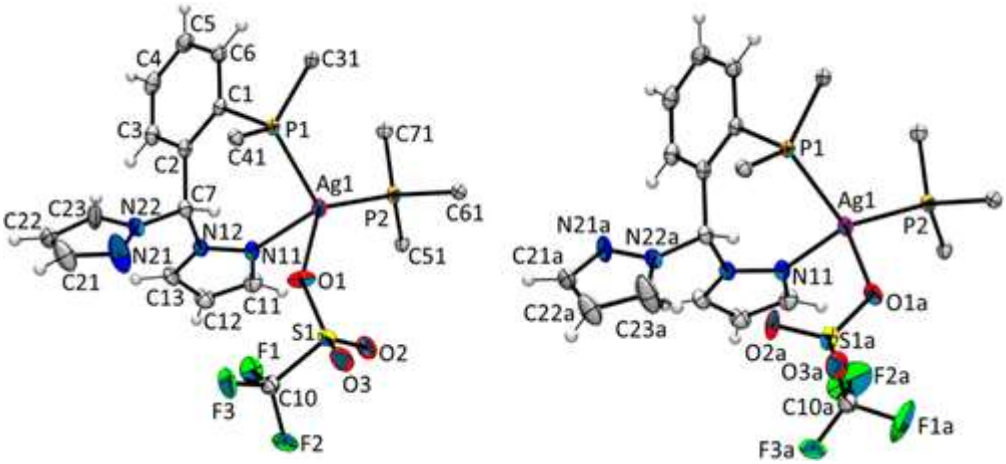

Figure 5. Views of two disorder components in the structure of [Ag(***o*L**)(PPh_3)](OTf), **4**, with atom labeling. Only the *ipso*-carbon atom bound to the phosphine atom on of the tolyl groups of ***o*L** and on the phenyl rings in PPh_3 are shown for clarity. Selected bond distances (Å): Ag1–P1 2.5060(6), Ag1–P2 2.4186(6), Ag1–N11 2.408(2), Ag1–O1 2.461(3), Ag1–O1a 2.323(17). Selected bond angles (°): P2–Ag1–P1 124.13(2), P2–Ag1–O1 131.42(7), O1–Ag1–P1 92.39(6), O1a–Ag1–P1 102.0(5), O1a–Ag1–P2 106.0(4), O1a–Ag1–N11 111.8(4), N11–Ag1–P1 105.25(5), N11–Ag1–P2 107.59(5), N11–Ag1–O1 89.19(8).

Supramolecular Structures

Aside from fundamental interest, the analysis of the supramolecular structures of complexes **1**·acetone, **2**·CH_3CN, **3**, and **5** is of importance to the interpretation of their solid state IR spectrum and potentially to the powder X-ray diffraction (PXRD) studies described later. The supramolecular structure of **1**·acetone is shown in

Figure 6 and is discussed below, while analyses of the other structures are provided in the Supporting Information. A feature common to the supramolecular structures of all the current complexes, and to most other Ag(OTf) complexes of di(pyrazolyl)methane ligands,[8a] is CH···O weak hydrogen bonding interactions[33] that occur between the triflate anion and the acidic methine and 5-pyrazolyl hydrogen atoms. That is, in **1**·acetone, a variety of weak CH···O hydrogen bonding interactions organize the 3D structure into stacked bilayer sheets with channels along the *b*-axis that hold solvent. Figure 6 shows only the shortest (sum of van der Waals radii −0.2 Å) and presumably strongest of these "intermolecular" CH···O interactions (cyan dashed lines), while Table 2 collects the metrics of these and of the longer interactions. Of the two independent triflate anions, that with S2 serves as a bridge to connect neighboring dications along the *a*-direction to form a dimer of dications (top right of Figure 6). That is, one of the oxygens (O4) interacts with Ag2 of one cation, while O5 acts as an acceptor in a bifurcated weak hydrogen bonding interaction with the methine (H57) and 5-pyrazolyl (H67) hydrogen donors of a neighboring dication with the metrics listed in Table 2. The third oxygen atom (O6) of this triflate anion participates in a long and presumably very weak noncovalent bonding interaction with a tolyl ring hydrogen (H85, *ortho*- to the methyl group). The Ag1–O1 bonds anchor two of the other independent triflate anions (that each contain S1) to the dimer of dications. The oxygen atom O3 of each "S1-containing" triflate acts as an acceptor in a bifurcated CH···O interaction with the methine hydrogen (H7) of neighboring dimer of dications as well as with a methyl group hydrogen (H3Sa) of an acetone solvate molecule. A bilayer sheet structure, that is one unit cell in width along the *a*-direction but infinite in the *bc*-plane (Figure 6), is formed since each dimer of dications contains two hydrogen donors and two acceptors of four C7H7···O3 interactions. The *bc*-sheets are further connected along the *a*-direction by two types of CH···O interactions involving the acetone solvate molecule. The first interaction, C3SH3Sa···O3, described previously, holds the acetone molecule to one sheet, while the oxygen atom of acetone (O1S) acts as an acceptor to a phenylene hydrogen (H6) that is *ortho*- to the ditolylphosphine group (top left of Figure 6) of an adjacent bilayer sheet. As a result of the sheet stacking, there are channels along the *b*-direction that contain acetone molecules as shown in the two views in the bottom of Figure 6.

Inorganic Chemistry, Vol 53, No. 22 (2014): pg. 12108-12121. DOI.

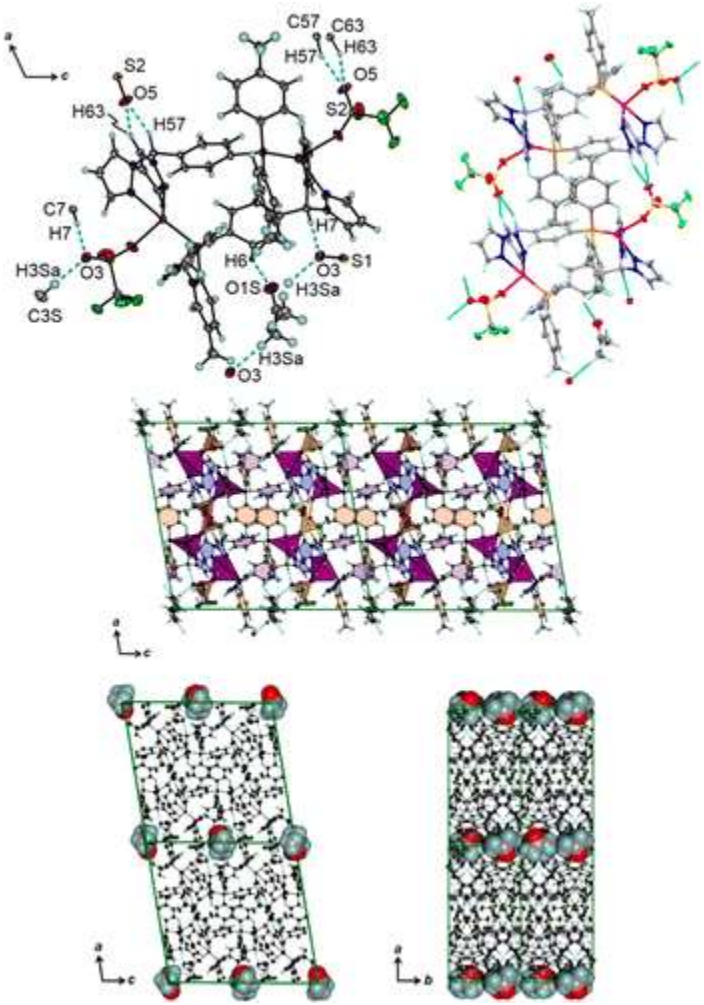

Figure 6. Supramolecular structure of **1**·0.5 acetone. Top left: View of CH···O interactions (cyan dashed lines); top right: Dimer formed by interactions involving only O5. Middle: View of *bc*-sheet bilayer structure (Ag as pink tetrahedra, triflate SO_3C unit as yellow tetrahedra, pyrazolyl rings as blue pentagons, phenylene linkers as violet hexagons; tolyl rings as orange hexagons); bottom: View of four unit cells down *b*- (left) and down *c*- (right) showing acetone filling channels along the *b*-direction.

Table 2. Geometries of C–H···O Weak Hydrogen-Bonding Interactions in **1**·acetone

Donor(D)(-H) ···Acceptor(A)	D–H (Å)	H···A (Å)	D···A (Å)	D–H···A (°)
C–H···O interactions				
C7–H7···O3	1.00	2.14	3.130(2)	169
C23–H23··· O1	0.95	2.53	3.368(2)	147
C57–H57···O5	1.00	2.21	3.119(2)	150
C63–H63···O5	0.95	2.40	3.133(2)	134
C85–H85··· O6	0.95	2.59	3.484(2)	158
C3S–H3Sa···O3	0.98	2.47	3.432(3)	169

Inorganic Chemistry, Vol 53, No. 22 (2014): pg. 12108-12121. DOI.

Donor(D)(-H) ···Acceptor(A)	D–H (Å)	H···A (Å)	D···A (Å)	D–H···A (°)
C6–H6···O1S	0.95	2.36	3.224(3)	151

It is important to note that each oxygen of both types of triflate ion in **1**·acetone (or of the anions in **2**·CH_3CN, **3**, **4**, or **5**, see Supporting Information) experiences a distinct (weak hydrogen-bonding) environment in the solid state. If the C–H···O interactions are significant, the local symmetry around either S1 or S2 in **1**·acetone could be effectively lowered to C_1 and give rise to an increase in the number and/or broadness of S–O stretches in the solid state IR spectrum (vide infra) compared to the idealized case where the local symmetry about sulfur in the CF_3SO_3 group is C_{3v}.

PXRD

Powder X-ray diffraction data were collected for the solid samples of **1**–**3** and **5** obtained immediately after their initial isolation (as-prepared samples are precipitated from THF and/or washed with Et_2O and dried under a vacuum), and after recrystallization from various solvents followed by drying under a vacuum. The PXRD patterns obtained for as-prepared samples of **5** match those calculated from single-crystal X-ray diffraction data (Figure S6, Supporting Information) which is expected since this compound crystallized without solvent in the lattice. This contrasts the situation for **2** where the diffraction pattern of the solvent-free (combustion analysis) powder does not match that calculated for the single crystal of **2**·CH_3CN (Figure S6), as might be expected. While X-ray diffraction quality crystalline blocks of **1**·0.5 acetone were obtained after allowing a layer of hexanes to diffuse into an acetone solution of **1**, vapor diffusion of Et_2O into an acetonitrile solution of **1** produces microcrystalline, ultrathin needles that are unsuitable for single crystal X-ray diffraction. Simply air drying these ultrathin needles is sufficient to give a solvent-free sample of **1** as determined by combustion analysis. Samples of air-dried needles of **1** (from CH_3CN) and those as-prepared samples of **1** from THF showed variable levels of crystallinity (middle and top of Figure 7, respectively). Given the supramolecular structure of **1**·0.5 acetone that showed solvent partly occupying channels, the ease of solvent removal, and the similarity of PXRD patterns, it is likely that the structures of the crystalline samples

Inorganic Chemistry, Vol 53, No. 22 (2014): pg. 12108-12121. DOI.

obtained from other solvent systems (i.e., especially the microcrystalline needles from CH_3CN) are closely related to that of **1**·0.5 acetone. Similarly, the crystal of **3** had heavily disordered solvent (Et_2O:CH_3CN) in large voids in the crystal (Supporting Information). Yet, the calculated PXRD pattern matched that of the as-isolated, solvent-free (combustion analysis) powder indicating that the overall structural features remain intact regardless of the presence or absence of solvent.

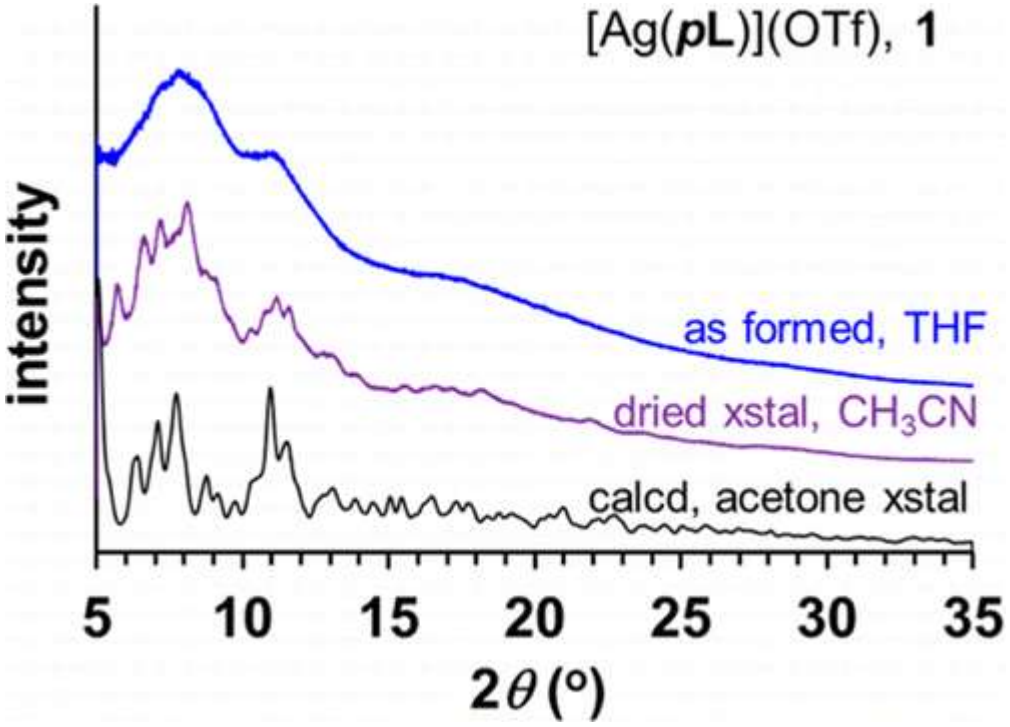

Figure 7. PXRD patterns obtained for samples of **1** obtained under various conditions compared to data (bottom) calculated from the single crystal diffraction data for **1**·0.5 acetone.

IR Spectra

The IR spectra of **1**–**4** and **5** in CH_3CN show characteristic bands for "unbound" or "ionic" triflate anions at 1271, 1157, 1093, and 966 cm^{-1}, for SO_3 and CF_3 stretching modes and combination bands,[34] but the solid state spectra are much more complicated than expected (Figure S7) presumably due to the various different weak CH···O interactions and, in the case of **1**, to the two crystallographically distinct types of triflate anions in the unit cell. For instance, single

Inorganic Chemistry, Vol 53, No. 22 (2014): pg. 12108-12121. DOI.

crystal X-ray diffraction of **5** shows tetracoordinate silver (τ_4 = 0.73, seesaw AgN_4 geometry, see Figure S1) due to binding only to pyrazolyl nitrogen donors. In this case, the triflate anion is not bound to the metal center, yet the solid-state IR spectrum is complicated. Examination of the supramolecular structure reveals that each of the three oxygens of the triflate participates in a different type of CH···O interaction (Figure S5) which may effectively lower the local symmetry of the SO_3 moiety and give rise to a greater than expected number of S–O stretches. The IR spectra of as-isolated powders of **1**–**4** and **5** are identical to those obtained for air-dried crystals; combustion analyses indicate that the powders or air-dried crystals are solvent-free.

Solution

NMR

The variable temperature multinuclear NMR and ESI(+) MS data (vide infra) indicate that, in solution at room temperature, compounds **1** and **2** likely maintain cyclic structures similar to the solid state, whereas the solution structures of **3** and **4** are different than their solid-state structures. The ^{31}P NMR spectral data of triarylphosphine silver(I) complexes are particularly useful for characterization as they can be diagnostic of the number and type of phosphine ligands bound to silver.[30,35] Silver has two naturally occurring NMR-active (I = 1/2) nuclei, ^{107}Ag (52% abundance) and ^{109}Ag (48% abundance). When silver is bound to one phosphorus atom, a characteristic set of doublet resonances such as shown in Figure 8a is expected. In the absence of exchange, the nearly overlapping doublets are resolved, and the ratio of one-bond coupling constants $^1J_{109Ag-P}/^1J_{107Ag-P}$ should be 1.15, corresponding to the ratio of the nuclear magnetic moments (μ_I, in nuclear magneton units, μ_N) μ_I (^{109}Ag) = −0.13056 μ_N: μ_I (^{107}Ag) = −0.11357 μ_N.[36] Typically, however, in complexes such as $[Ag(PPh_3)_n]^+$ (n = 1–4) the solution exchange is rapid at room temperature so the doublet resonances are not resolved; they only become resolved at low temperature (below 203 K).[35b] The ^{31}P NMR spectra of **1** and **2** in CD_3CN are remarkable in that the doublet resonances are resolved at room temperature, indicative of slow exchange on the NMR time scale. In fact, resolution of the two doublets for $^{109/107}$Ag–P coupling is lost due to exchange broadening only after heating CD_3CN solutions of **1** to

Inorganic Chemistry, Vol 53, No. 22 (2014): pg. 12108-12121. DOI.

60 °C or of **2** to 40 °C. At room temperature, the $^{1}J_{107Ag-P}$ coupling constant of 638 Hz for **1** and 644 Hz for **2**, is comparable to other silver complexes with only one phosphine bound to silver such as $(Ph_3P)Ag(NO_3)$ (780 Hz),[30a] $(Ph_3P)Ag(PF_6)$ (755 Hz),[35b] and $(tBu_3P)Ag(NO_3)$ (683 Hz),[35d] or to other complexes binding one phosphine and pyrazolyl donors such as $[(Ph_3P)Ag(pz_6C_6)](SbF_6)$ (648 Hz),[37] $[(\eta^5\text{-}C_5Me_5)1r(pz)_3Ag(PPh_3)]$ (565 Hz),[38] or $[HB(pz)_3]Ag(PPh_3)$ (607 Hz).[39] Silver complexes bound to two phosphines have much smaller $^{1}J107_{Ag-P}$ coupling constants in the 400–500 Hz range such as 496 Hz for $[(p\text{-}tolyl_3P)_2Ag]PF_6$,[35b] 507 Hz for $[(Ph_3P)_2Ag](PF_6)$,[35b] and 432 Hz for $[(tBu_3P)_2Ag](NO_3)$.[35d] Thus, neither **1** nor **2** isomerize in solution to give a species where one silver is bound to two phosphines and the other silver is only bound to pyrazolyls (like Figure 1e). A second line of evidence that a cyclic structure is preserved in solution at room temperature comes from the ^{1}H NMR data of **2**. The downfield portion of the spectrum and labeling scheme are shown on the right of Figure 8. Although we verified assignments of hydrogen resonances in ***mL*** and **2** by 2D NMR (NOESY, COSY) experiments, the aryl hydrogen resonances (both the tolyl and central phenylene) of **2** can be assigned by simple inspection by considering relative integration, the asymmetric nature of the ligand that gives different distinctive multiplicities to the central phenylene resonances ($H_{e\text{-}h}$, Figure 8), and by the different magnitudes of the hydrogen–phosphorus coupling constants. The doublet resonance at 5.6 ppm ($^{3}J_{H-P}$ = 9.5 Hz) for the single hydrogen atom, H_e, situated between the phosphorus and the methine carbon, is highly shielded compared to other resonances or to that of the free ligand at 6.8 ppm ($^{3}J_{H-P}$ = 7.1 Hz) in the same solvent. Inspection of the solid state structure of **2** (Figure 3b) shows that this H_e hydrogen is sandwiched between the π-clouds of both a tolyl group and a pyrazolyl ring. Upon warming the solution to 60 °C, the doublet resonance for H_e becomes deshielded and exhibits the greatest downfield shift (of 0.2 ppm) compared with other resonances. The resonance for the tolyl hydrogens, H_i, close to the phosphorus atom, experiences the next greatest shift of 0.1 ppm downfield, followed by the resonance for H_f (the other phenylene hydrogen *ortho*- to P) which shifts upfield by 0.06 ppm. The resonances for pyrazolyl hydrogens only shift by 0.01 ppm over the same temperature range. Thus, the environment around the phosphorus atom exhibits the greatest change with temperature, perhaps being indicative of dissociation at

Inorganic Chemistry, Vol 53, No. 22 (2014): pg. 12108-12121. DOI.

high temperature. Interestingly, there is only one set of resonances for each pyrazolyl and tolyl group in the ^{1}H NMR spectrum of either **1** or **2**, even at low temperature (233 K for CD_3CN, 193 K in acetone-d_6). Two sets of resonances for tolyl group hydrogens and two sets of resonances for pyrazolyl hydrogens were expected based on the solid state structures of the complexes that showed distinct "axial" and "equatorial" rings of each type. Thus, while the low temperature ^{31}P NMR data (and ^{1}H NMR data for **2**) indicate that the metallacycles are intact, the 18- and 16-member metallacycles of **1** and **2**, respectively, must have low barriers to inversion that would allow facile exchange axial and equatorial pyrazolyl or tolyl rings. Reger and co-workers have recently demonstrated similar dynamic behavior in metallacycles supported by related *m*-pz$_4$xyl.[7b,7e]

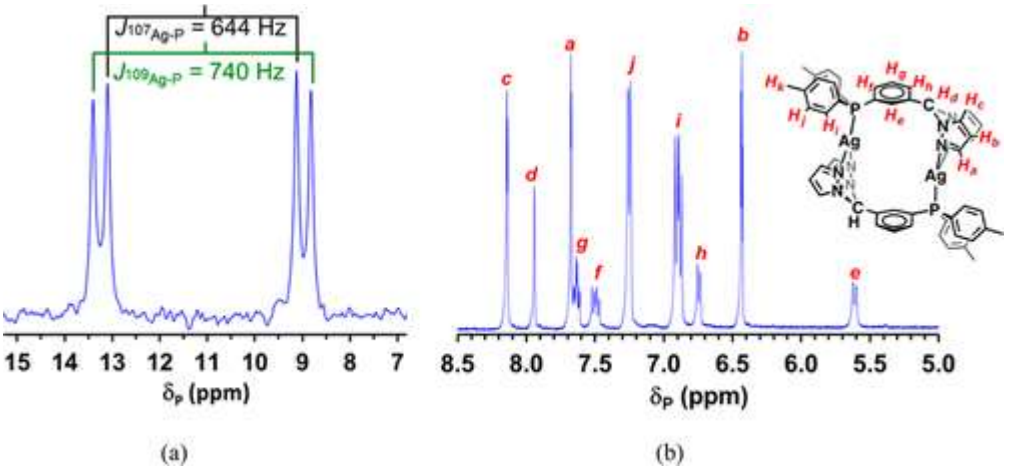

Figure 8. (a) ^{31}P NMR spectrum of [Ag(***m*L**)](OTf), **2**, in CD_3CN at 295 K and (b) downfield portion of the ^{1}H NMR spectrum of **2** with atom labeling scheme.

In contrast to the above, the ^{31}P NMR spectrum of **3** in CD_3CN shows only a broad singlet at room temperature due to (intermediate) exchange. Upon lowering the temperature to 273 K, the coalescence temperature is reached, and the resonance appears as a broad doublet. Two doublet resonances for ^{109}Ag–P and ^{107}Ag–P coupling are only partially resolved at 233 K, near the freezing point of the solvent, where the $^{1}J_{^{107}Ag-P}$ coupling constant of ca. 580 Hz is in line with other complexes with one phosphine bound to silver, as described above. It is of interest that the energy barrier to exchange (indicated by loss of Ag–P coupling) decreases with increasing steric bulk around the phosphorus atom of the ligand in the complexes in the order: **3** < **2** <

Inorganic Chemistry, Vol 53, No. 22 (2014): pg. 12108-12121. DOI.

1. Such a trend further implicates that exchange occurs by dissociation of the phosphine.

Finally, the ^{31}P NMR spectrum of **4** in acetone-d_6 (Figure 9) at room temperature consists of two broad singlet resonances near δ_P +11 ppm and −3 ppm, for the phosphorus nuclei of the PPh_3 ligand and the P(*p*-tolyl)$_2$ moiety, respectively. Such an assignment is based on the observation that the difference between the chemical shift of the resonance for a silver(I) triarylphosphine complex and that for the free triarylphosphine ligand, $\Delta\delta_P = \delta_P(\text{complex}) - \delta_P(\text{ligand})$, is typically on the order of +20 ppm.[39] In this case, free PPh_3 and the free ligand resonate at δ_P −6 and −20 ppm, respectively, giving $\Delta\delta_P$ of 17 ppm for each type of phosphine. For reference, the $\Delta\delta_P$ for **1**–**3** were 19, 18, and 19 ppm, respectively. At low temperature, each singlet resonance of **4** resolves into two overlapping doublet of doublet resonances due to ^{109}Ag–P, ^{107}Ag–P, and P–P coupling as illustrated in the top of Figure 9. The $^1J_{107Ag-P}$ coupling constant of 484 Hz for the PPh_3 moiety and of 396 Hz for the P(*p*-tolyl)$_2$ moiety are in the expected 400–500 Hz range for bis(triaryl)phosphine complexes, as outlined earlier. Moreover, the two different types of phosphorus lead to a $^2J_{P-P}$ coupling of 108 Hz, which is larger than 26 Hz found in $[PhB(CH_2PPh_2)_3]Ag(PEt_3)$[40] but is on par with 134 Hz found for $\{[\mu\text{-}(\eta^5\text{-}C_5H_4)PPh_2]Ag(PPh_3)\}_2$.[41] At intermediary temperatures (213 K to ca. 253 K) other resonances are observed in the baseline of the ^{31}P NMR spectrum (between 10 to 5 ppm and near 0 ppm), but their low intensity and the low signal-to-noise ratio prevented definitive assignment of these presumed intermediates or equilibrium species.

Inorganic Chemistry, Vol 53, No. 22 (2014): pg. 12108-12121. DOI.

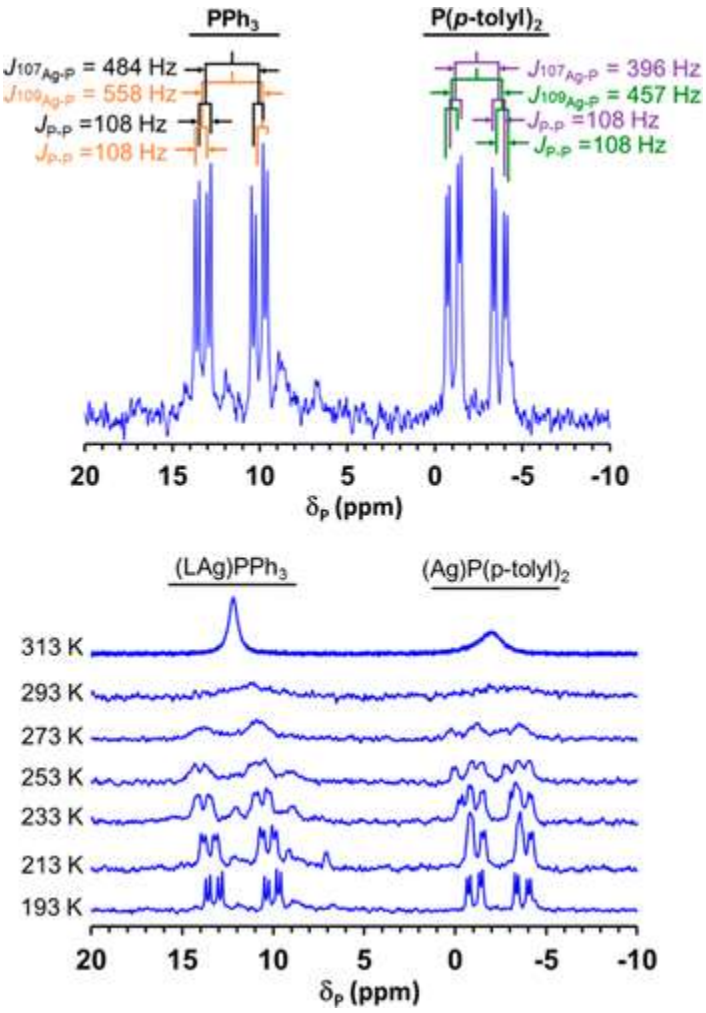

Figure 9. Top: ^{31}P NMR spectrum of [Ag(***o*L**)(PPh_3)](OTf), **4**, in acetone-d_6 at 193 K. Bottom: overlay of spectra of **4** in acetone-d_6 acquired at different temperatures.

ESI(+) Mass Spectrometry

Complexes **1**–**3** as CH_3CN solutions were characterized by ESI(+) mass spectrometry. The parent (100%) peak for **1** occurred at m/z = 544 for the $[Ag_2L_2]^{2+}$ dication. The identity of the dication versus an $[AgL]^+$ cation is easily determined by examination of the isotope pattern, especially since the former shows half-integer peaks, as in the right of Figure 10. Careful inspection of the intensities of the experimental data for the peaks near m/z = 544 of **2** (most notably by the peaks at m/z = 543 and 547, right of Figure 10) reveals that they deviate slightly from the theoretical values for $[Ag_2L_2]^{2+}$ because about 5–10% of the total signal in this region is for [Ag(***m*L**)]$^+$. The spectra

Inorganic Chemistry, Vol 53, No. 22 (2014): pg. 12108-12121. DOI.

of **1** and **2** also show a low abundance peak (1–2%) at *m*/*z* = 1237 for $[Ag_2L_2(OTf)]^+$, providing further evidence for the persistence of the metallacycles under these conditions. In the spectrum of **3**, the parent peak is at *m*/*z* = 979 for $[AgL_2]^+$. The second most abundant peak occurs at *m*/*z* = 584 for $[(\textbf{\textit{oL}})Ag(CH_3CN)]^+$. A low abundance (5%) peak found at *m*/*z* = 543 is for the monocation $[AgL]^+$. Collectively, the data indicate that **3** is extensively dissociated under these conditions rather than being polymeric akin to the complexes' solid state structure.

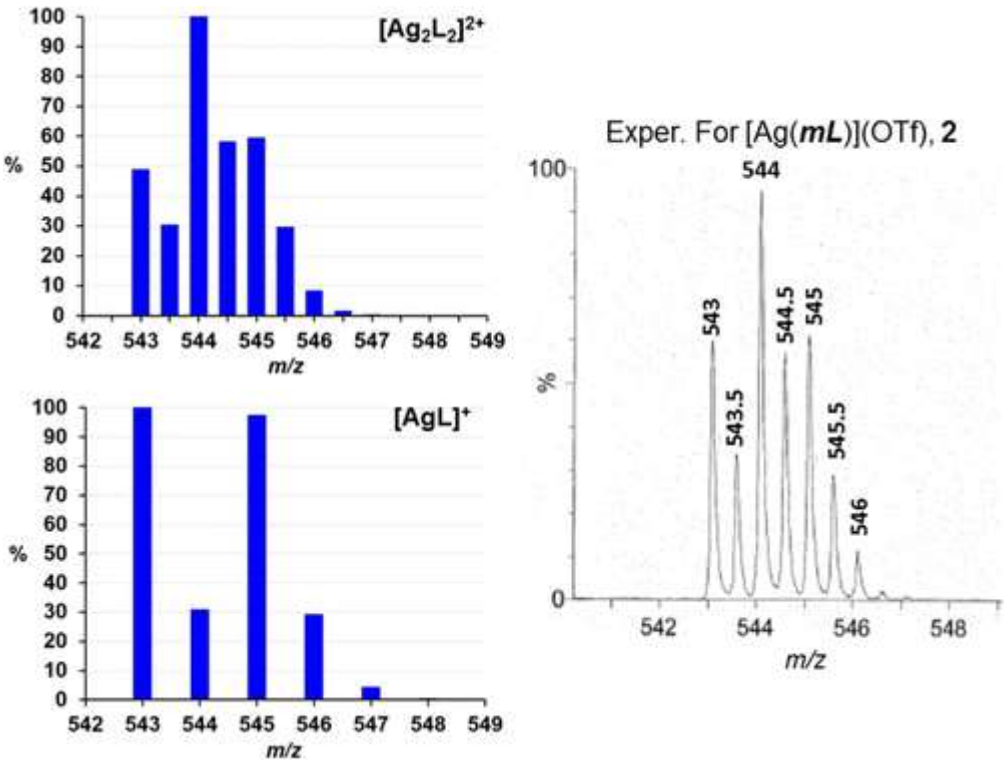

Figure 10. Comparison of theoretical isotope pattern for $[AgL]^+$, $[Ag_2L_2]^{2+}$, and the experimental pattern for **2**.

Summary and Conclusions

Silver(I) trifluoromethanesulfonate complexes of the newly prepared heteroditopic ligands containing di(*p*-tolyl)phosphine and di(pyrazolyl)methane groups bound to a phenylene spacer give different solid state and solution structures depending on the juxtaposition of the donor moieties. A coordination polymer, **3**, is formed in the solid state if the donors are situated *ortho*- to one

Inorganic Chemistry, Vol 53, No. 22 (2014): pg. 12108-12121. DOI.

another on the phenylene ring. However, when the groups are disposed either *para*- (as in **1**) or *meta*- (as in **2**), the resultant silver complexes have cyclic bimetallic dications with 18- and 16-membered metallacyclic rings, respectively. In crystals of **1**·0.5 acetone, **2**·CH_3CN, and **3**, the supramolecular structure was organized mainly by CH···O interactions involving the triflate oxygen and the acidic methine and 5-pyrazolyl hydrogens. The persistence of the cyclic structures of each **1** and **2** in CH_3CN is evident by the ~640 Hz one-bond Ag–P coupling in the room-temperature ^{31}P NMR spectrum, the variable temperature ^{1}H NMR spectrum of **2**, and the ESI(+) mass spectrum of **1** and **2**. The ^{31}P NMR data for **1** and **2** are particularly remarkable because one-bond Ag–P coupling is not observed in the room temperature spectrum of **3**, $[Ag(PR_3)_n]^+$ (n = 1–4), or most other heteroleptic $[LAgP]^{n+}$ complexes due to the lability of the Ag–P bond or bonds between other donors and silver. Evidently cyclic structures slow the rate of exchange, an observation that may have use in the future design of shape-persistent supramolecular assemblies of silver(I). The combination of NMR and ESI(+) mass spectral data for **3** suggests that the coordination polymer is likely extensively dissociated in CH_3CN. Insight into the possible solution structure of **3** in CH_3CN was gleaned by exploring the reaction between **3** and the strong Lewis donor PPh_3, which gave a monomeric Lewis adduct **4** that showed a chelating κ^2-*P,N* ligand in the solid state. The solution structure of **4** was dynamic where exchange involving phosphine could only be stopped at very low temperature (193 K in acetone-d_6). Future studies on the reactivity of these ligands and their silver(I) complexes toward transition metal salts is underway in our laboratory.

The authors declare no competing financial interest.

References

[1](a) Foo, M. L.; Matsuda, R.; Kitagawa, S. Chem. Mater. 2014, 26, 310– 322. (b) Li, J.-R.; Kuppler, R. J.; Zhou, H.-C. Chem. Soc. Rev. 2009, 38, 1477– 1504. (c) Férey, G. Chem. Soc. Rev. 2008, 37, 191– 214. (d) Maji, T. K.; Kitagawa, S. Pure Appl. Chem. 2007, 79, 2155– 2177. (e) Lee, J. Y.; Olson, D. H.; Pan, L.; Emge, T. J.; Li, J. Adv. Funct. Mater. 2007, 17, 1255– 1262

[2](a) Wei, L.; Wei, Q.; Lin, Z.-E.; Meng, Q.; He, H.; Yang, B.-F.; Yang, G.-Y. Angew. Chem., Int. Ed. 2014, 53, 7188– 7191. (b) Heine, J.; Mueller-Buschbaum, K. Chem. Soc. Rev. 2013, 42, 9232– 9242. (c) Xu, C.;

Zhang, Z.-Y.; Ren, Z.-G.; Zhou, L.-K.; Li, H.-X.; Wang, H.-F.; Sun, Z.-R.; Lang, J.-P. Cryst. Growth Des. 2013, 13, 2530– 2539. (d) Cui, Y.; Yue, Y.; Chen, B. Chem. Rev. 2012, 112, 1126– 1162

[3](a) Butler, K. T.; Hendon, C. H.; Walsh, A. J. Am. Chem. Soc. 2014, 136, 2703– 2706. (b) Nafady, A.; O'Mullane, A. P.; Bond, A. M. Coord. Chem. Rev. 2014, 268, 101– 142. (c) Givaja, G.; Amo-Ochoa, P.; Gomez-Garcia, C. J.; Zamora, F. Chem. Soc. Rev. 2012, 41, 115– 147. (d) Gomez-Herrero, J.; Zamora, F. Adv. Mater. 2011, 23, 5311– 5317. (e) Zhang, W.; Ye, H.-Y.; Xiong, R.-G. Coord. Chem. Rev. 2009, 253, 2980– 2997. (f) Janiak, C. Dalton Trans. 2003, 14, 2781– 2804. (g) Chen, C. T.; Suslick, K. S. Coord. Chem. Rev. 1993, 128, 293– 322

[4](a) Wang, L.; Wang, W.; Di, S.; Yang, X.; Chen, H.; Gong, T.; Zhou, S. RSC Adv. 2014. (b) Tan, H.; Zhang, L.; Ma, C.; Song, Y.; Xu, F.; Chen, S.; Wang, L. ACS Appl. Mater. Interfaces 2013, 5, 11791– 11796. (c) Lu, X.; Cheng, H.; Huang, P.; Yang, L.; Yu, P.; Mao, L. Anal. Chem. 2013, 85, 4007– 4013. (d) Novio, F.; Simmchen, J.; Vazquez-Mera, N.; Amorin-Ferre, L.; Ruiz-Molina, D. Coord. Chem. Rev. 2013, 257, 2839– 2847. (e) Tabacaru, A.; Pettinari, C.; Marchetti, F.; di Nicola, C.; Domasevitch, K. V.; Galli, S.; Masciocchi, N.; Scuri, S.; Grappasonni, I.; Cocchioni, M. Inorg. Chem. 2012, 51, 9775– 9788

[5](a) Li, L.; Matsuda, R.; Tanaka, I.; Sato, H.; Kanoo, P.; Jeon, H. J.; Foo, M. L.; Wakamiya, A.; Murata, Y.; Kitagawa, S. J. Am. Chem. Soc. 2014, 136, 7543– 7546. (b) Cook, T. R.; Zheng, Y.-R.; Stang, P. J. Chem. Rev. 2013, 113, 734– 777. (c) Wang, C.; Liu, D.; Lin, W. J. Am. Chem. Soc. 2013, 135, 13222– 13234. (d) Zhao, D.; Timmons, D. J.; Yuan, D.; Zhou, H. C. Acc. Chem. Res. 2011, 44, 123– 133. (e) Ranocchiari, M.; van Bokhoven, J. A. Phys. Chem. Chem. Phys. 2011, 13, 6388– 6396. (f) Uemura, T.; Yanai, N.; Kitagawa, S. Chem. Soc. Rev. 2009, 38, 1228– 1236. (g) Kitagawa, S.; Kitaura, R.; Noro, S.-i. Angew. Chem., Int. Ed. 2004, 43, 2334– 2375

[6](a) Mukherjee, A.; Tothadi, S.; Desiraju, G. R. Acc. Chem. Res. 2014. (b) Bombicz, P.; Gruber, T.; Fischer, C.; Weber, E.; Kalman, A. CrystEngComm 2014, 16, 3646– 3654. (c) Cherukuvada, S.; Guru Row, T. N. Cryst. Growth Des. 2014, 14. (d) Cavallo, G.; Metrangolo, P.; Pilati, T.; Resnati, G.; Terraneo, G. Cryst. Growth Des. 2014, 14, 2697– 2702. (e) Goesten, M. G.; Kapteijn, F.; Gascon, J. CrystEngComm 2013, 15, 9249– 9257. (f) Mastalerz, M. Nat. Chem. 2013, 5, 810– 811. (g) Siddiqui, K. A.; Tiekink, E. R. T. Chem. Commun. 2013, 49, 8501– 8503. (h) Desiraju, G. R. J. Am. Chem. Soc. 2013, 135, 9952– 9967. (i) Du, M.; Li, C.-P.; Liu, C.-S.; Fang, S.-M. Coord. Chem. Rev. 2013, 257, 1282– 1305. (j) Aakeröy, C. B.; Panikkattu, S. V.; DeHaven, B.; Desper, J. Cryst. Growth Des. 2012, 12, 2579– 2587. (k) Aakeröy, C. B.; Champness, N.; Janiak, C.

CrystEngComm 2010, 12, 22– 43. (l) Braga, D. Chem. Commun. 2003, 2751– 2754. (m) Aakeröy, C. B. Acta Crystallogr., Sect. B: Struct. Sci. 1997, 53, 569– 586. (n) Desiraju, G. R. Angew. Chem., Int. Ed. 1995, 34, 2311– 2327

[7](a) Reger, D. L.; Watson, R. P.; Smith, M. D. Inorg. Chem. 2006, 45, 10077– 10087. (b) Reger, D. L.; Pascui, A. E.; Pellechia, P. J.; Smith, M. D.; Jezierska, J.; Ozarowski, A. Inorg. Chem. 2014, 53, 4325– 4339. (c) Reger, D. L.; Pascui, A. E.; Foley, E. A.; Smith, M. D.; Jezierska, J.; Ozarowski, A. Inorg. Chem. 2014, 53, 1975– 1988. (d) Reger, D. L.; Pascui, A. E.; Pellechia, P. J.; Ozarowski, A. Inorg. Chem. 2013, 52, 12741– 12748. (e) Reger, D. L.; Pascui, A. E.; Pellechia, P. J.; Smith, M. D. Inorg. Chem. 2013, 52, 11638– 11649. (f) Reger, D. L.; Pascui, A. E.; Smith, M. D.; Jezierska, J.; Ozarowski, A. Inorg. Chem. 2012, 51, 11820– 11836

[8](a) Gardinier, J. R.; Tatlock, H. M.; Hewage, J. S.; Lindeman, S. V. Cryst. Growth Des. 2013, 13, 3864– 3877. (b) Durá, G.; Carrión, M. C.; Jalón, F. A.; Manzano, B. R.; Rodríguez, A. M. Eur. J. Inorg. Chem. 2013, 5943– 5957

[9](a) Durá, G.; Carrión, M. C.; Jalón, F. A.; Rodríguez, A. M.; Manzano, B. R. Cryst. Growth Des. 2014, 14, 3510– 3529. (b) Durá, G.; Carrión, M. C.; Jalón, F. A.; Rodríguez, A. M.; Manzano, B. R. Cryst. Growth Des. 2013, 13, 3275– 3282. (c) Carrión, M. C.; Durá, G.; Jalón, F. A.; Manzano, B. R.; Rodríguez, A. M. Cryst. Growth Des. 2012, 12, 1952– 1969

[10](a) Santillan, G. A.; Carrano, C. J. Dalton Trans. 2009, 6599– 6605. (b) Santillan, G. A.; Carrano, C. J. Cryst. Growth Des. 2009, 9, 1590– 1598. (c) Santillan, G. A.; Carrano, C. J. Inorg. Chem. 2008, 47, 930– 939. (d) Santillan, G. A.; Carrano, C. J. Dalton Trans. 2008, 3995– 4005

[11](a) Bassanetti, I.; Mezzadri, F.; Comotti, A.; Sozzani, P.; Gennari, M.; Calestani, G.; Marchiò, L. J. Am. Chem. Soc. 2012, 134, 9142– 9145. (b) Bassanetti, I.; Marchiò, L. Inorg. Chem. 2011, 50, 10786– 10797

[12](a) Reger, D. L.; Watson, R. P.; Gardinier, J. R.; Smith, M. D. Inorg. Chem. 2004, 43, 6609– 6619. (b) Reger, D. L.; Gardinier, J. R.; Grattan, T. C.; Smith, M. R.; Smith, M. D. New J. Chem. 2003, 27, 1670– 1677. (c) Reger, D. L.; Brown, K. J.; Gardinier, J. R.; Smith, M. D. Organometallics 2003, 22, 4973– 4983. (d) Reger, D. L.; Gardinier, J. R.; Semeniuc, R. F.; Smith, M. D. Dalton Trans. 2003, 9, 1712– 1718

[13]Li, Q.; Xie, Y.-F.; Sun, B.-C.; Yang, J.; Song, H.-B.; Tang, L.-F. J. Organomet. Chem. 2013, 745–746, 106– 114

[14](a) Bassanetti, I.; Gennari, M.; Marchiò, L.; Terenghi, M.; Elviri, L. Inorg. Chem. 2010, 49, 7007– 7015. (b) Gennari, M.; Bassanetti, I.; Marchiò, L. Polyhedron 2010, 29, 361– 371.

[15]Morin, T. J.; Merkel, A.; Lindeman, S. V.; Gardinier, J. R. Inorg. Chem. 2010, 49, 7992– 8002

[16](a) Bassanetti, I.; Marchiò, L. Inorg. Chem. 2011, 50, 10786– 10797. (b) Ding, K.; Cheng, C.-H.; Yang, Y.-X.; Song, H.-B.; Tang, L.-F. J. Organomet. Chem. 2011, 696, 3662– 3667. (c) Blasberg, F.; Bats, J. W.; Bolte, M.; Lerner, H.-W.; Wagner, M. Inorg. Chem. 2010, 49, 7435– 7445. (d) Peters, L.; Hübner, E.; Haas, T.; Heinemann, F. W.; Burzlaff, N. J. Organomet. Chem. 2009, 694, 2319– 2327. (a) Chandrasekhar, V.; Thilagar, P.; Senapati, T. Eur. J. Inorg. Chem. 2007, 1004– 1009. (f) Otero, A.; Fernandez-Baeza, J.; Antinolo, A.; Carrillo-Hermosilla, F.; Tejeda, J.; Lara-Sanchez, A.; Sanchez-Barba, L.; Fernandez-Lopez, M.; Rodriguez, A. M.; Lopez-Solera, I. Inorg. Chem. 2002, 41, 5193– 5202

[17]Coulson, D. R.; Satek, L. C.; Grim, S. O. Inorg. Synth. 1990, 28, 107– 109

[18]CrysAlisPro, Agilent Technologies,Version 1.171.34.46 (release 25-11-2010 CrysAlis171.NET), (compiled Nov 25 2010, 17:55:46).

[19]Olex2 1.2 (compiled 2013.11.15 svn.r2834 for OlexSys, GUI svn.r4720). Dolomanov, O. V.; Bourhis, L. J.; Gildea, R. J.; Howard, J. A. K.; Puschmann, H. J. Appl. Crystallogr. 2009, 42, 339– 341

[20]Sheldrick, G. M. SHELXTL, Version 6.12; Bruker Analytical X-ray Systems, Inc.: Madison Wisconsin, USA, 2001.

[21](a) Thé, K. I.; Peterson, L. K. Can. J. Chem. 1973, 51, 422– 426. (b) Thé, K. I.; Peterson, L. K.; Kiehlmann, E. Can. J. Chem. 1973, 51, 2448– 2451. (c) Peterson, L. K.; Kiehlmann, E.; Sanger, A. R.; Thé, K. I. Can. J. Chem. 1974, 52, 2367– 2374

[22]Liddle, B. J.; Hall, D.; Lindeman, S. V.; Smith, M. D.; Gardinier, J. R. Inorg. Chem. 2009, 48, 8404– 8414

[23]Stein, R. A.; Knobler, C. Inorg. Chem. 1977, 16, 242– 245

[24](a) Terrobaa, R.; Hursthouse, M. B.; Laguna, M.; Mendiac, A. Polyhedron 1999, 18, 807– 810. (b) Bardají, M.; Crespo, O.; Laguna, A.; Fischer, A. K. Inorg. Chim. Acta 2000, 304, 7– 16

[25]Teo, B.-K.; Calabrese, J. C. Inorg. Chem. 1976, 15, 2467– 2474

[26]For example: Argyle, V. J.; Woods, L. M.; Roxburgh, M.; Hanton, L. R. CrystEngComm 2013, 15, 120– 134

[27]CSD Version 5.35, November 2013.

[28]Yang, L.; Powell, D. R.; Houser, R. P. Dalton Trans. 2007, 955– 964

[29]The closest Ag1···O3 distance in **2**·CH_3CN is 3.796 Å; there is a longer Ag1···F2 contact of 3.1068(19) Å that is less than 3.24 Å, the sum of van der Waals radii, but this contact is best classified as a secondary interaction.

[30]See for example: (a) Barron, P. F.; Dyason, J. C.; Healy, P. C.; Engelhardt, L. M.; Skelton, B. W.; White, A. H. J. Chem. Soc., Dalton Trans. 1986, 1965– 1970. (b) Cingolani, A.; Effendy; Hanna, J. V.; Pellei, M.;

Pettinari, C.; Santini, C.; Skelton, B. W.; White, A. H. Inorg. Chem. 2003, 42, 4938– 4948. (c) Bachman, R. E.; Andretta, D. F. Inorg. Chem. 1998, 37, 5657– 5663 and references

[31](a) Zartilas, S.; Hadjikakou, S. K.; Hadjiliadis, N.; Kourkoumelis, N.; Kyros, L.; Kubicki, M.; Baril, M.; Butler, I. S.; Karkabounas, S.; Balzarini, J. Inorg. Chim. Acta 2009, 362, 1003– 1010. (b) Omondi, B.; Venter, G. J. S.; Roodt, A.; Meijboom, R. Acta Crystallogr. 2009, B65, 699– 706. (c) Venter, G. J. S.; Roodt, A.; Meijboom, R. Acta Crystallogr. 2009, B65, 182– 188. (e) Venter, G. J. S.; Meijboom, R.; Roodt, A. Acta Crystallogr., Sect. E 2006, 62, m3453– m3455. (f) Camalli, M.; Caruso, F. Inorg. Chim. Acta 1987, 127, 209– 213

[32](a) Pellei, M.; Alidori, S.; Papini, G.; Lobbia, G. G.; Gorden, J. D.; Dias, H. V. R.; Santini, C. Dalton Trans. 2007, 42, 4845– 4853. (b) Dias, H. V. R.; Alidori, S.; Lobbia, G. G.; Papini, G.; Pellei, M.; Santini, C. Inorg. Chem. 2007, 46, 9708– 9714. (c) Santini, C.; Pellei, M.; Alidori, S.; Lobbia, G. G.; Benetollo, F. Inorg. Chim. Acta 2007, 360, 2121– 2127. (d) Pettinari, C.; Cingolani, A.; Lobbia, G. G.; Marchetti, F.; Martini, D.; Pellei, M.; Pettinari, R.; Santini, C. Polyhedron 2004, 23, 451– 469

[33](a) Wheeler, S. E.; Bloom, J. W. G. J. Phys. Chem. A 2014. (b) Bernstein, J. Cryst. Growth Des. 2013, 13, 961– 964. (c) Gu, Y.; Kar, T.; Scheiner, S. J. Am. Chem. Soc. 1999, 121, 9411– 9422. (d) Desiraju, G. J. Acc. Chem. Res. 1996, 29, 441– 449. (e) Steiner, T.; Saenger, F. J. Am. Chem. Soc. 1992, 114, 10146– 10154. (f) Desiraju, G. J. Acc. Chem. Res. 1991, 24, 290– 296. (g) Taylor, R.; Kennard, O. J. Am. Chem. Soc. 1982, 104, 5063– 5070

[34](a) Lawrance, G. A. Chem. Rev. 1986, 86, 17– 33. (b) Grochala, W.; Cyránski, M. K.; Derzsi, M.; Michałowski, T.; Malinowski, P. J.; Mazej, Z.; Kurzydłowski, D.; Kózmínski, W.; Budzianowskia, A.; Leszczýnski, P. J. Dalton Trans. 2012, 41, 2034– 2047

[35](a) Meijboom, R.; Bowen, R. J.; Berners-Price, S. J. Coord. Chem. Rev. 2009, 253, 325– 342 and references. (b) Chen, F.; Oh, S.-W.; Wasylishen, R. E. Can. J. Chem. 2009, 87, 1090– 1101. (c) Alyea, E. C.; Malito, J.; Nelson, J. H. Inorg. Chem. 1987, 26, 4294– 4296. (d) Goel, R. G.; Pilon, P. Inorg. Chem. 1978, 17, 2876– 2879. (e) Muetterties, E. L.; Alegranti, C. W. Inorg. Chem. 1972, 94, 6386– 6391

[36]CRC Handbook of Chemistry and Physics, 95th ed.; Haynes, W. M., Ed.; CRC Press: Boca Raton, FL, 2014–2015; Section 11, 55– 56; http://www.hbcpnetbase.com (accessed August 5, 2014) .

[37]Caballero, A.; Guerrero, A.; Jalón, F. A.; Manzano, B. R.; Claramunt, R. M.; María, M. D. S.; Escolástico, C.; Elguero, J. Inorg. Chim. Acta 2003, 347, 168– 174

[38]Carmona, D.; Oro, L. A.; Lamata, M. P.; Jimeno, M. L.; Elguero, J.; Belguise, A.; Lux, P. Inorg. Chem. 1994, 33, 2196– 2203

[39]Santini, C.; Lobbia, G. G.; Pettinari, C.; Pellei, M.; Valle, G.; Calogero, S. Inorg. Chem. 1998, 37, 890– 900

[40]McCain, M. N.; Schneider, S.; Salata, M. R.; Marks, T. J. Inorg. Chem. 2008, 47, 2534– 2542

[41]Lettko, L.; Rausch, M. D. Organometallics 2000, 19, 4060– 4065

Supporting Information for

Isomer Dependence in the Assembly and Lability of Silver(I) Trifluoromethanesulfonate Complexes of the Heteroditopic Ligands 2-, 3-, and 4-[di(1H-pyrazolyl)methyl]phenyl(di-p-tolyl)phosphine.

James R. Gardinier*, Jeewantha S. Hewage, and Sergey V. Lindeman

Table of Contents:

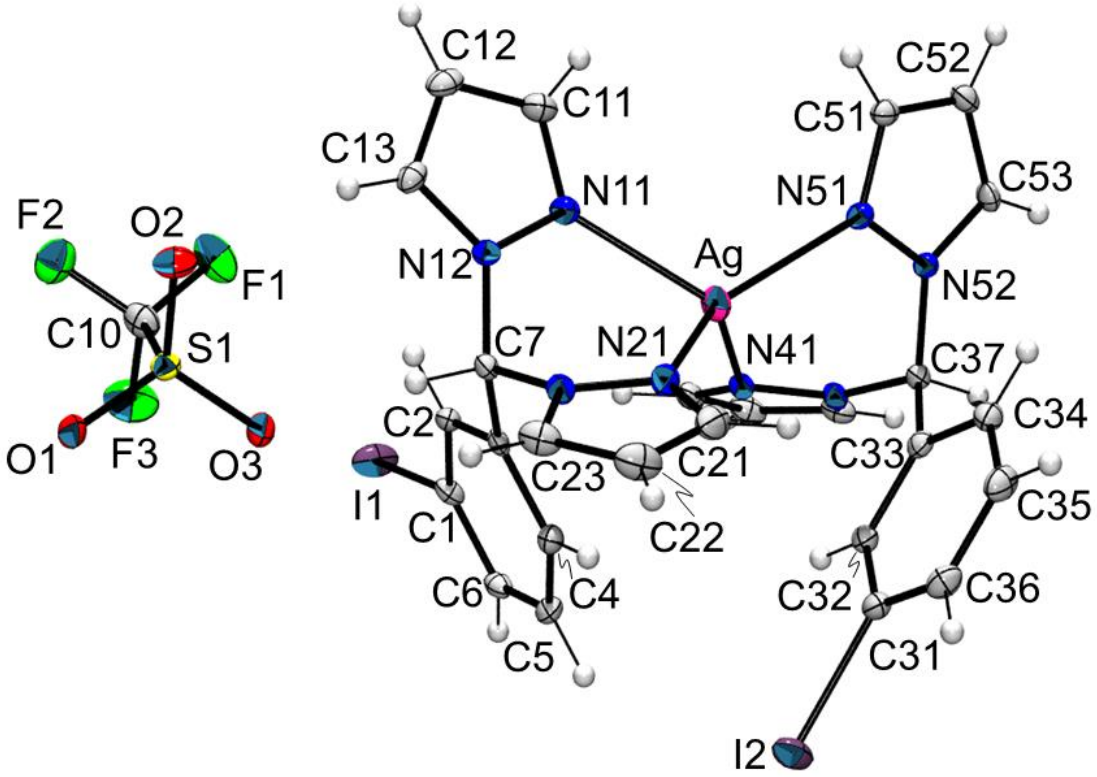

Figure S1. Structure of [(*m*-$IC_6H_4CHpz_2)_2Ag$](OTf), **5**. Selected bond distances (Å): Ag1-N11 2.314(3), Ag1-N21 2.269(3), Ag1-N41 2.326(3), Ag1-N51 2.263(2). Selected bond angles (°): N11-Ag1-N41 113.21(9), N21-Ag1-N11 85.52(9), N21-Ag1-N41 128.40(9), N51-Ag1-N11 119.72(9), N51-Ag1-N21 128.05(9), N51-Ag1-N41 85.20(8).

Details of Cambridge Structural data base (CSD) Search.

(a) Ag···OSO_2CF_3 interactions. The query shown in Scheme S1 drawn in the ConQuest version 1.15 software package[S1] was used in the search of Cambridge Structural Database,

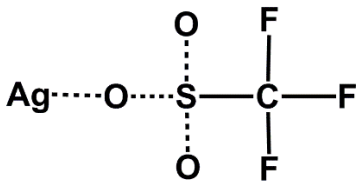

Scheme S1. Diagram used in query of CSD search.

version 5.35 (updates November 2013). The bonds between Ag and O as well as those between S and O were set to "any", indicated by the dashed lines in Scheme S1. Those bonds between S and C and between C and F were single. This search produced 432 "hits" (CSD refcodes) with a total of 1047 entries due to multiple entries (Ag-O interactions) per hit. A histogram showing the bond distance distribution of the 1047 entries is found in Figure S2. The minimum distance was 2.075 Å, the maximum was 3.017 Å, the mean was 2.48 Å, the median was 2.47 Å and the standard deviation was 0.13 Å.

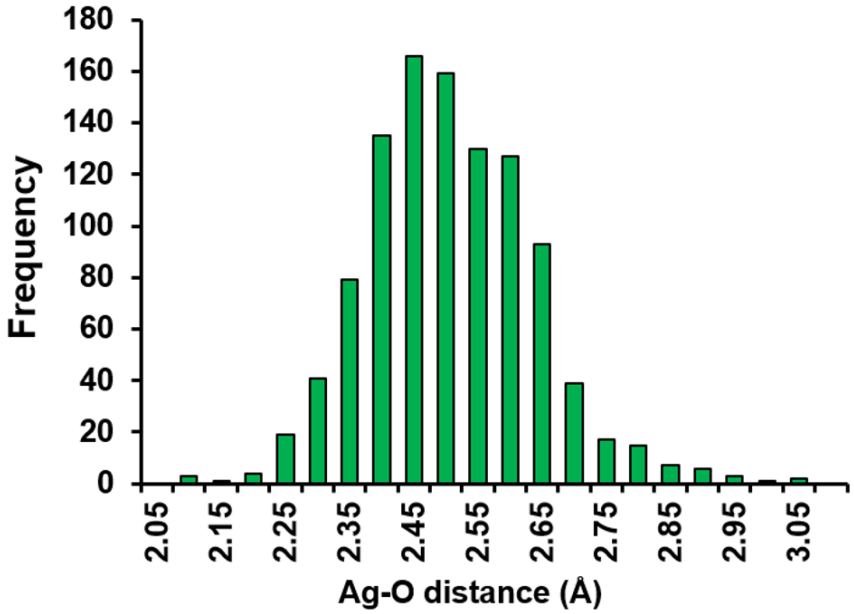

Figure S2. Histogram showing distribution of Ag-O distances (A).

Supramolecular Structures.

[Ag(***mL***)](OTf)·CH_3CN, **2·CH_3CN**. Figure S3 and Table S1 provide illustrations and metrics of the noncovalent interactions that organize **2**·CH_3CN into a 3D layered sheet structure. The CH···O[S2]

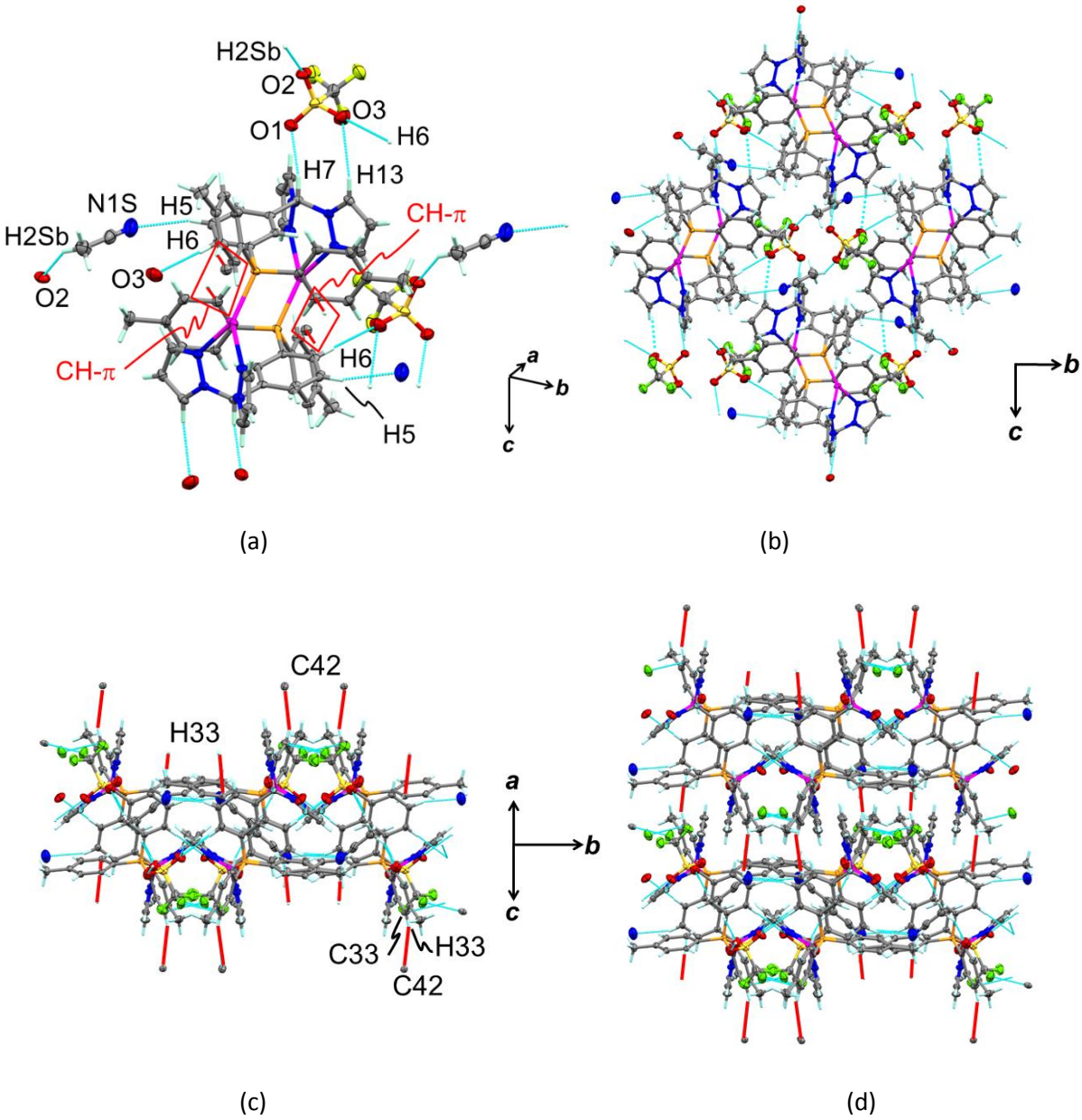

Figure S3. Supramolecular structure of **2**·CH_3CN. (a) view of CH···O interactions (cyan lines) and CH···π interactions (red lines) that organize the structure and atom labeling. (b) View down *a*- axis of four **2**·CH_3CN units in a sheet showing only CH···O interactions. (c) Same four units but viewed perpendicular to *b*-axis and with CH···π interactions (highlighted as red lines). (d) Two sheets stacked by CH···π interactions.

Table S1. Geometries of weak C-H···(X= O[S2], N[S2f,S3]) and C-H···π[S4] interactions in [Ag(***mL***)](OTf) CH_3CN, **2** CH_3CN.

Donor(D)(-H) ···Acceptor(A)	D-H (Å)	H···A (Å)	D···A (Å)	D-H···A (°)	γ(°)
C-H···X interactions					
C7-H7···O1	1.00	2.16	3.126(3)	163	
C6-H6··· O3	0.95	2.50	3.452(3)	177	
C13-H13···O3	0.95	2.59	3.474(3)	155	
C2S-H2Sb···O2	0.98	2.37	3.231(4)	147	
C5-H5··· N1s	0.95	2.54	3.439(4)	159	
C-H···π interaction					
C33-H33···Ct(N41)	0.95	2.56	3.502(3)	170	5.4
Ct(*i*) = centroid of ring containing atom *i*; γ = Angle CH-Ct(*i*) and normal to plane containing Ct(*i*)					

Interactions between the triflate oxygen atoms and acidic hydrogens of the dication serve to assemble sheets in the *bc*- plane (cyan lines, Fig S3a-c). That is two oxygen atoms (O1 and O3) of a triflate anion are anchored to the neighboring methine and 5-pyrazolyl hydrogens (H7 and H13, respectively) of a dication. The oxygen atom O3 participating in the interaction with the 5-pyrazolyl (H13) also interacts with a phenylene hydrogen, H6, situated *ortho*- to the phosphorus (and para- to the dipyrazolylmethyl) of a neighboring dication. A sheet parallel with the *bc*- plane is formed (Fig S3b-c) as a result of the inversion symmetry of the dication that gives two H6 donors and two O3 acceptors per unit of **2**. Acetonitrile is anchored to the sheet by a CH···O interaction[S2] between the third oxygen, O2, of the triflate and a methyl hydrogen, H2Sb, of the solvate molecule as well as a CH···Ninteraction[S2f, S3] between the nitrogen, N1s, of CH_3CN and the phenylene hydrogen, H5, that is positioned meta- to both the phosphorus and the $CHpz_2$ moiety. Finally the *bc*- sheets are stacked along the *a*- direction by C-H···π interaction[S4] (red lines, Figs S3c and d) between a tolyl hydrogen, H33, ortho to the tolyl methyl) of one sheet and a pyrazolyl ring containing N41 of a neighboring sheet (the shortest contact is actually with C42 of the pz ring).

[Ag(***oL***)](OTf), **3**. Figure S4 illustrates the noncovalent interactions that govern the assembly of the polymer chains in **3** in three dimensions while Table S2 details the geometry of the (sub) van der Waals contacts. As described in the main text (see Fig. 4), **3** forms a coordination polymer that propagates

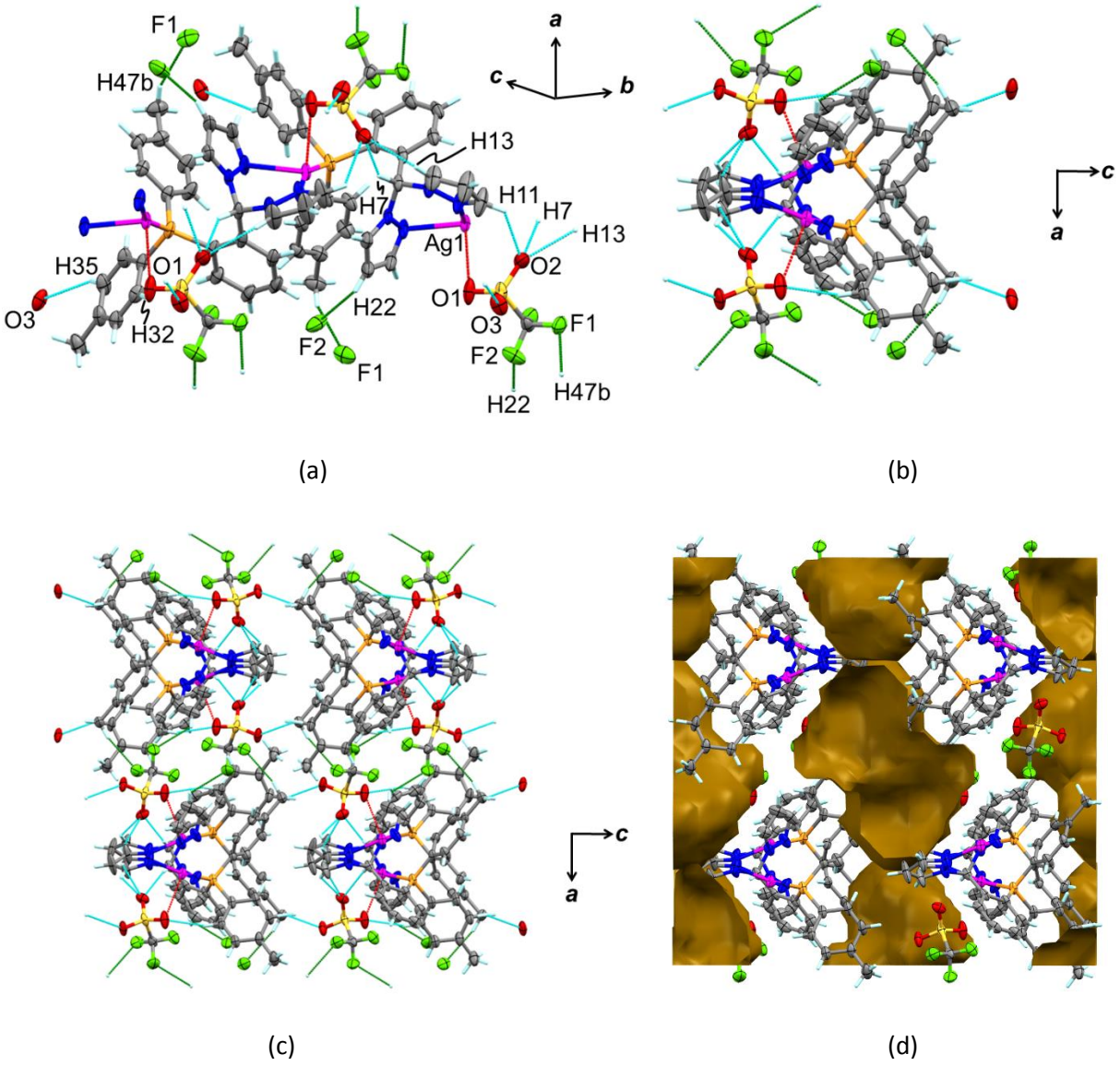

(a) (b)

(c) (d)

Figure S4. Supramolecular structure of [Ag(***oL***)](OTf), **3**. (a) View of coordination polymer with short contacts (CH···O cyan lines, CH···F green lines) and atom labeling. (b) View of coordination polymer down *b*- axis. (c) Representation of crystal packing diagram viewed down the *b*-axis with short noncovalent contacts highlighted as in (a). (d) View of one unit cell showing voids where disordered Et_2O:CH_3CN reside.

Table S2. Geometries of short C-H···(X=O, F[S5]) contacts in [Ag(***oL***)](OTf), **3**.

Donor(D)(-H) ···Acceptor(A)	D-H (Å)	H···A (Å)	D···A (Å)	D-H···A (°)
C-H···O interactions (Σ vdW -0.2 Å)				
C7-H7···O2	1.00	2.25	3.117(3)	144
C11-H11··· O2	0.95	2.51	3.134(5)	123
C13-H13···O2	0.95	2.43	3.146(4)	132
C32-H32···O1	0.95	2.43	3.299(4)	152
C-H···O interactions (Σ vdW -0.1 Å)				
C35-H35··· O3	0.95	2.61	3.434(4)	145
C-H···F vdW limit contacts				
C47-H47b···F1	0.98	2.58	3.509(4)	159
C22-H22···F2	0.95	2.62	3.293(4)	128

with the *b*- axis. The triflate anion is bound to the cationic polymer backbone by a relatively long Ag···O contact (Ag1-O1 2.809(3) Å, red lines, Figure S4a and Fig. 4, main text) and is held further by four short "intrachain" CH···O interactions that are 0.2 A less than the sum of the van der Waals radii of H and O (Table S2, cyan lines Fig. S4). That is O2 of the anion is involved in a trifurcated CH···O interaction with the methine and 5-pyrazolyl hydrogen atoms (H7, H13) of one monomer unit and with the 3-pyrazolyl hydrogen, H11, of the neighboring monomer unit in the polymer chain. The fourth intrachain CH···O interaction occurs with O1 (that is also in contact with Ag) and a tolyl ring hydrogen that is *ortho* to phosphorus. The chains are connected along the c- direction to form sheets parallel with the bc-plane by a longer (Σ vdW -0.1 Å) C-H···O interaction between the third oxygen of the triflate, O3, of one chain and a tolyl ring hydrogen, H35, meta- to phosphorus of a neighboring chain. The *bc*- sheets are stacked along the c- direction such that there are two short CH···F contacts (green lines, Fig. S4) that are just shorter than 2.67 Å, the sum of the van der Waals radii of H and F. The first contact occurs between the triflate fluorine F1 and a tolyl methyl hydrogen, H47b while the second occurs between F2 and a 4-pyrazolyl hydrogen, H22. This assembly leaves large voids (Fig. S4d) in the unit cell accounting for 1064 out of 8487 $Å^3$ or 16.4% of the total cell volume. Heavily disordered solvent mixture (approximately 1:1 CH3CN Et2O) reside in the voids. These are easily removed on drying in air or under vacuum.

Figure S5 labels the atoms and centroids of various short non-covalent interactions that organize the supramolecular structure of [(*m*-IC$_6$H$_4$CHpz$_2$)$_2$Ag](OTf), **5**; the metrics are listed in Table S3.

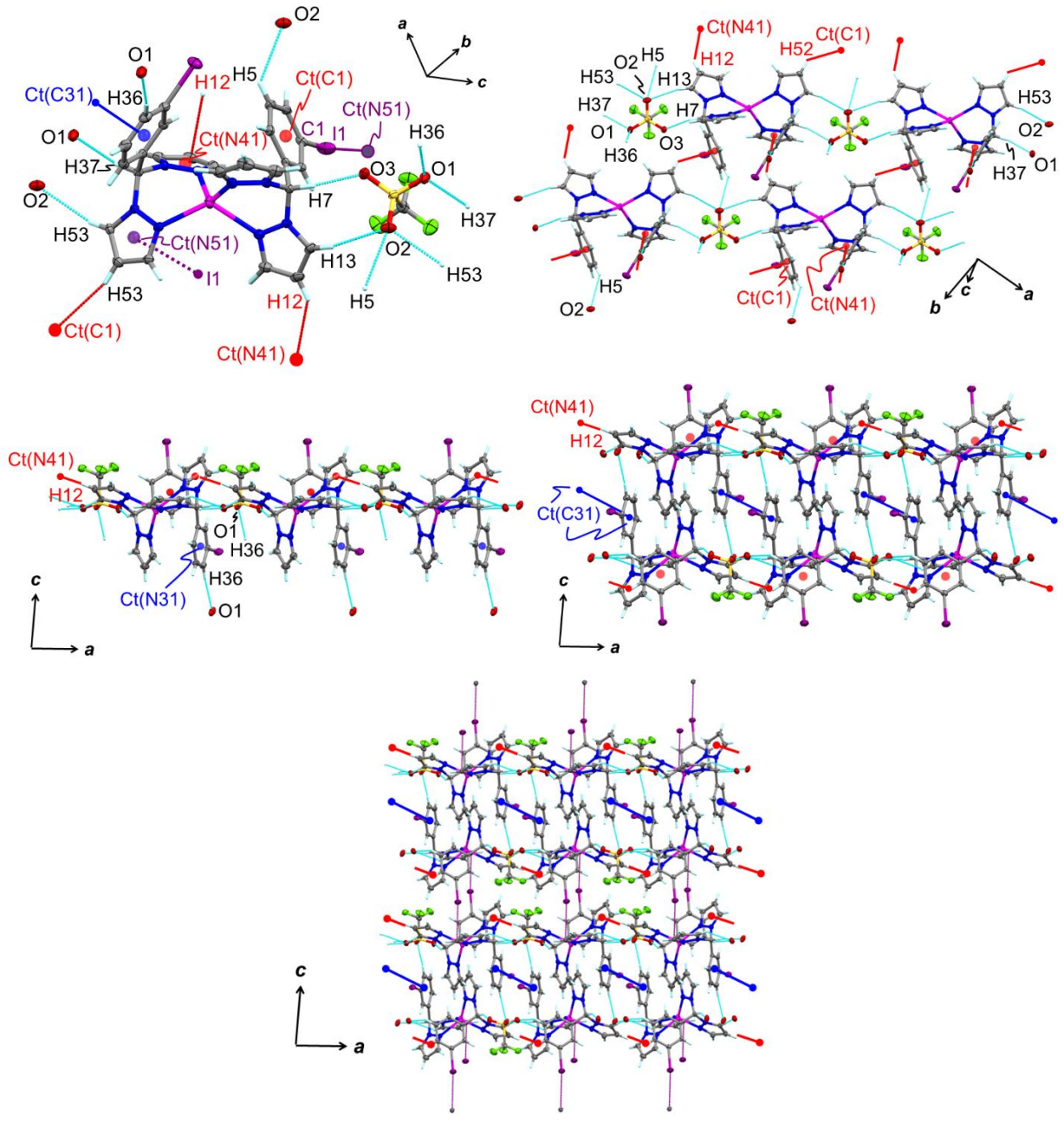

Figure S5. Supramolecular structure of [(*m*-IC$_6$H$_4$CHpz$_2$)$_2$Ag](OTf), **5**. Top left: View of asymmetric unit with labeling of important contacts (C-H···O, cyan; C-H···π, red; π···π, blue; C-I···π, purple). Top right: View of one layer perpendicular to *ab*- plane. Middle left: View of one layer down *b*-axis. Middle right: View down b- axis of bilayer sheet. Bottom: Stacking of two bilayer sheets giving short C-I···π contacts (purple vertical lines).

Table S3. Summary of short contacts and non-covalent interactions organizing the supramolecular structure of [(*m*-$IC_6H_4CHpz_2)_2Ag$](OTf), **5**.

$\pi\cdots\pi$[S6]	Ct-Ct	$\perp_{Avg}$ Dist (Å)	α(°)	β(°)	γ(°)
Ct(C31)-Ct(C31)	3.816(2)	3.472 (1)	0	24.5	24.5
Donor(D)-X ⋯Acceptor(A)	D-X (Å)	X⋯A (Å)	D⋯A (Å)	D-X⋯A (°)	γ(°)
C12-H12⋯Ct(N41)	0.95	2.80	3.585(3)	140	13.0
C52-H52⋯Ct(C1)	0.95	2.79	3.540(4)	136	9.6
C36-H36⋯O1	0.95	2.39	3.332(4)	173	
C37-H37⋯O1	1.00	2.13	3.116(4)	167	
C5-H5⋯O2	0.95	2.56	3.246(4)	129	
C13-H13⋯O2	0.95	2.48	3.411(4)	165	
C53-H53⋯O2	0.95	2.55	3.376(4)	146	
C7-H7⋯O3	1.00	2.08	3.015(4)	155	
C1-I1⋯Ct(N51)	2.094(3)	3.5580(13)	5.616(3)	166.61(8)	12.3

Ct(*i*) = centroid of ring containing atom i; α = dihedral angle between mean planes x and y. β = Angle Ct(*i*)-Ct(*j*); γ = Angle Ct(*i*)-Ct(*j*) and normal to plane containing Ct(*j*); $\perp_{Avg}$ Dist = average of perpendicular distance of centroid *i* to ring *j* and of centroid *j* to ring *i*.

There are six C-H⋯O interactions (cyan lines Fig. S5) that hold triflate anions to cations. Five of the C-H⋯O interactions assemble ions into a sheet structure that lies parallel with the *ab*- plane. Thus, neighboring methine and 5-pyrazolyl hydrogens (H7 and H13, respectively) serve as donors to O3 and O2 acceptors, respectively, of a triflate anion, attaching ions by two points. The ion pair is assembled into a polymer cahin along the a- direction by a similar set of C-H⋯O interactions involving the methine (H37) and 5-pyrazolyl (H53) hydrogens on the other side of the cation which interact with O1 and O2 of a neighboring ion pair. The polymer chains are assembled along *b*- into a sheet structure by the interaction between O2 and the phenylene hydrogen (H5) *meta*- to both the iodine atom, I1, and the $CHpz_2$ group (top right Fig. S5). Two CH-π interactions between two 4-pyrazolyl donors (H12 and H52) and a pyrazolyl (containing N41) or an iodophenyl (containing C1) further support the sheet structure. Two sheets are held together into a bilayer by the sixth C-H⋯O interaction between O1 of one sheet and a phenylene hydrogen, H35, that is *ortho*- to iodine (I2) but *para*- to a $CHpz_2$ moiety on an neighboring sheet. A π-π interaction[S6] (blue lines, Fig S5) between two iodophenyl groups that contain I2 further supports the bilayer. The bilayers are stacked along the *c*- axis in manner such that there is a short contact (purple lines Fig S5) between I1 and a pyrazolyl carbon C51 of 3.50 Å that is nearly 0.2 Å shorter than 3.68 Å, the sum of the van der Waals radii of C and I.

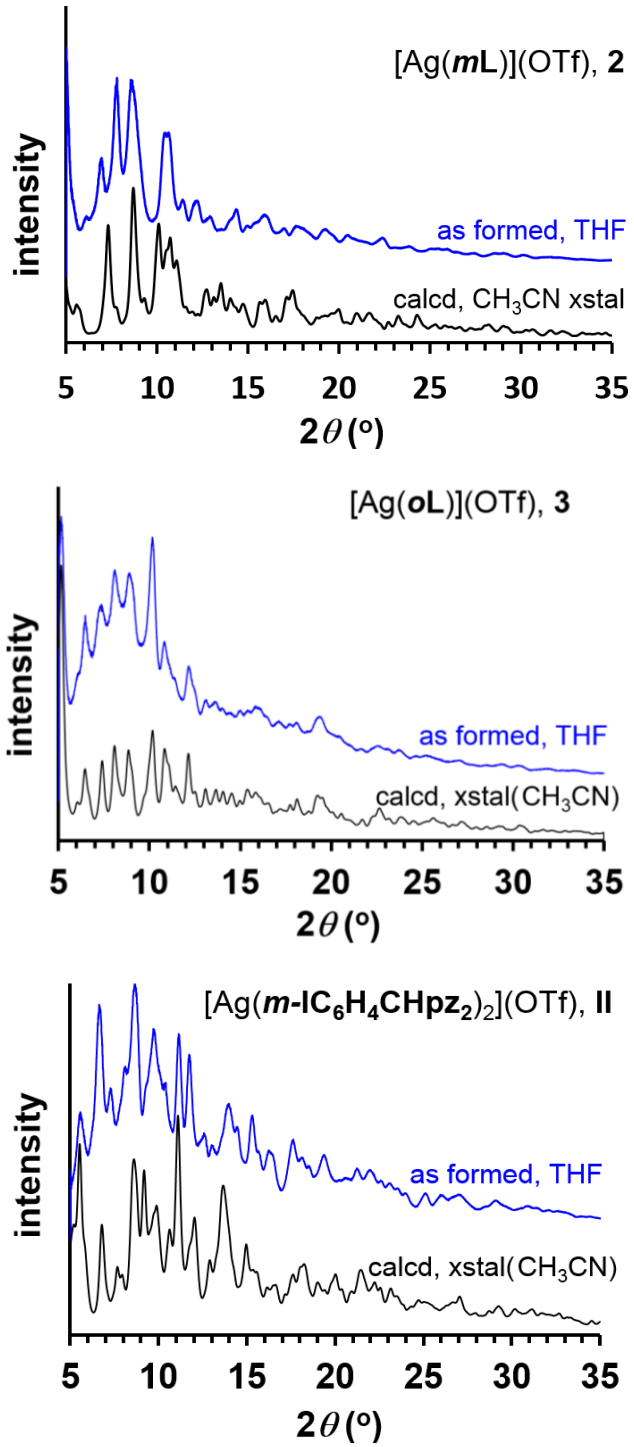

Figure S6. X-ray Powder Diffraction Patterns for samples of samples of **2**, **3**, and **5** obtained directly after work-up (prior to recrystallization) and comparison with patterns calculated from single crystal X-ray diffraction studies.

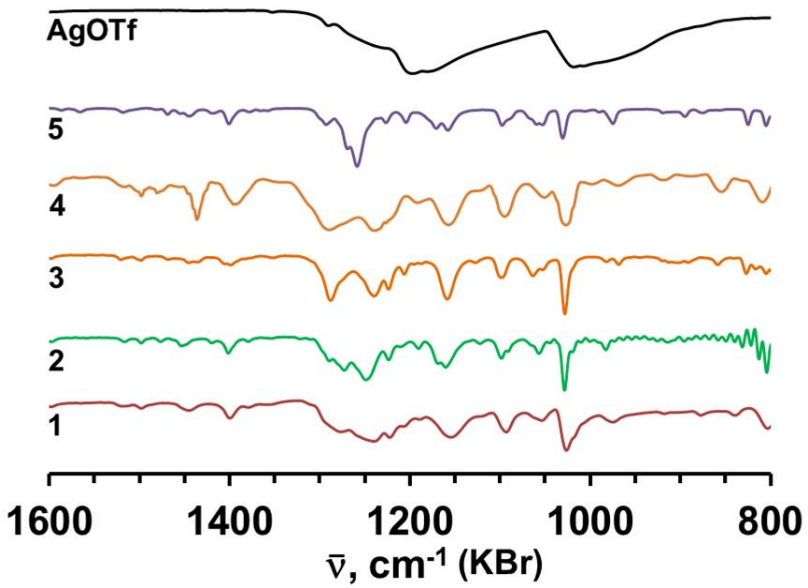

Figure S7. Portion of the IR spectrum obtained for solid samples of **1**-**4**, and **5** as KBr pellets.

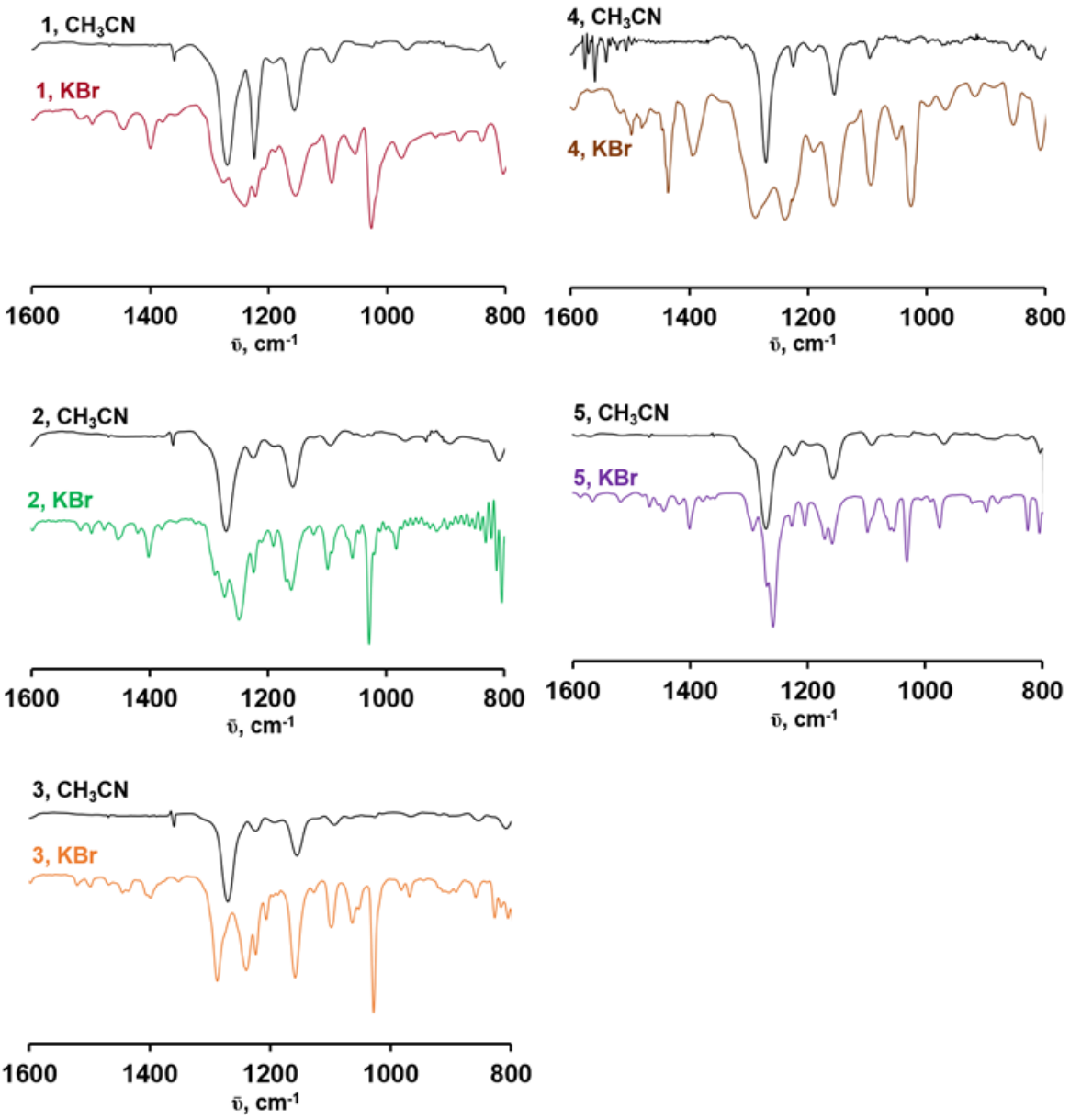

Figure S8. Comparison of portion (in the S-O and C-F stretching region) of IR spectra of each **1**-**5** in CH_3CN versus solid samples.

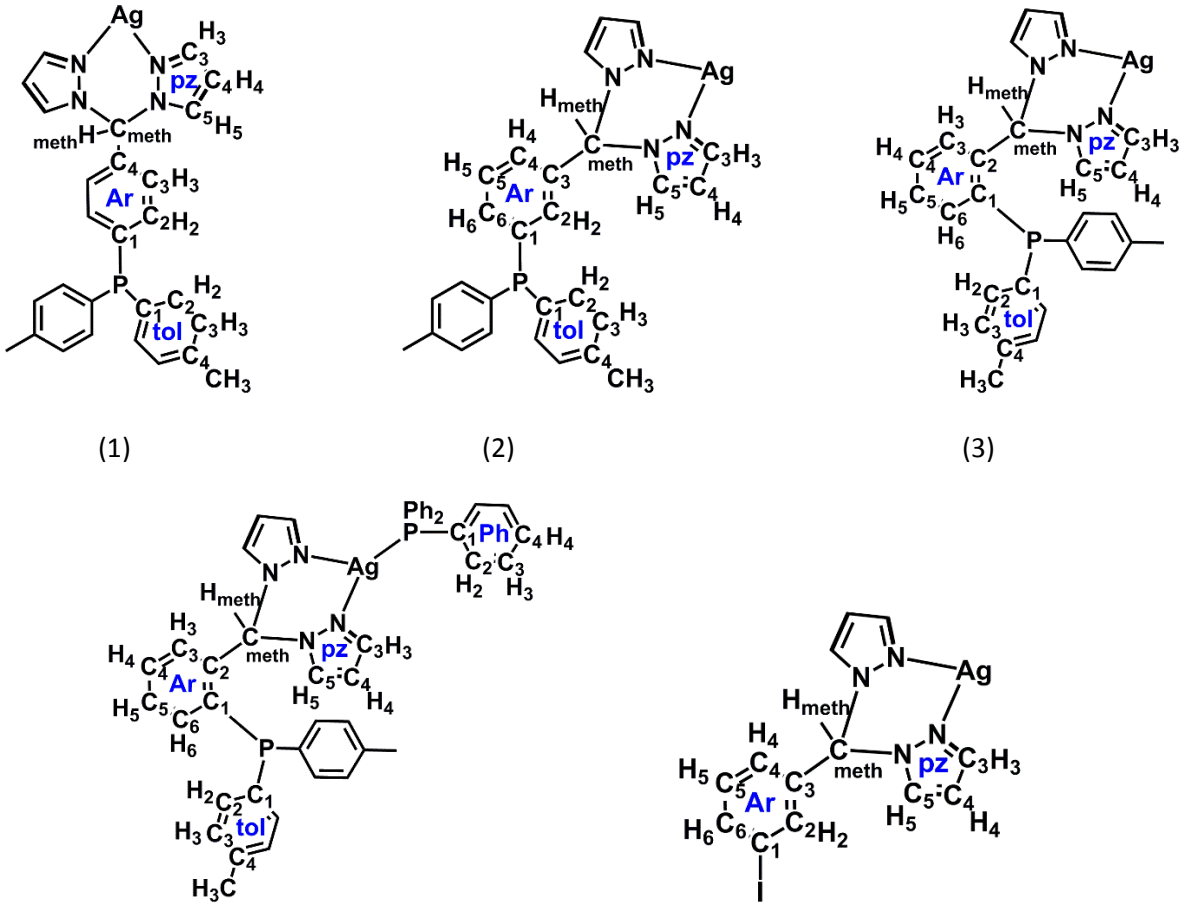

Figure S9. Atom labeling diagrams of **1**-**5** used in experimental section for NMR assignments.

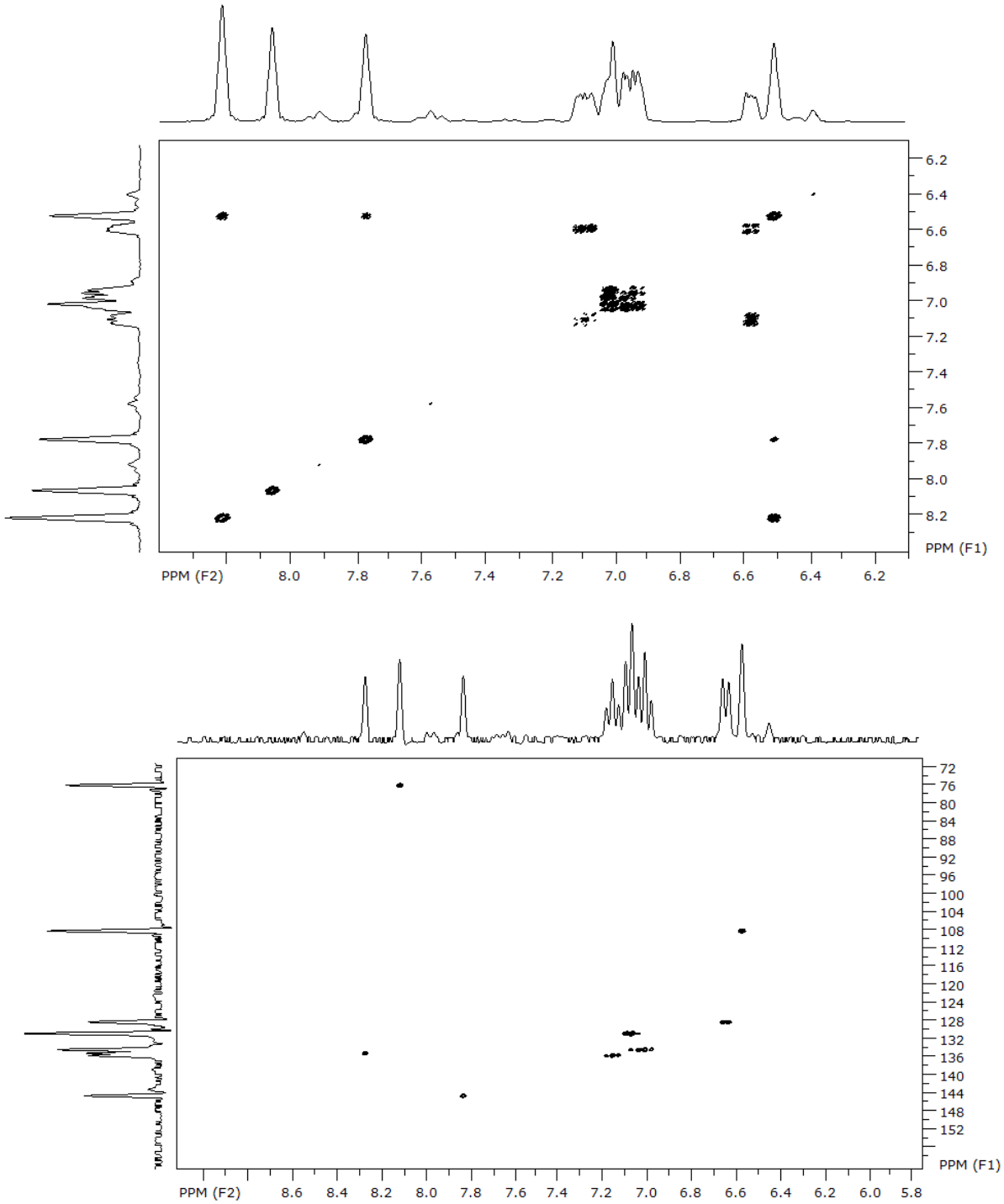

Figure S10. COSY (top) and HMQC (bottom) spectra of **1** in CD_3CN.

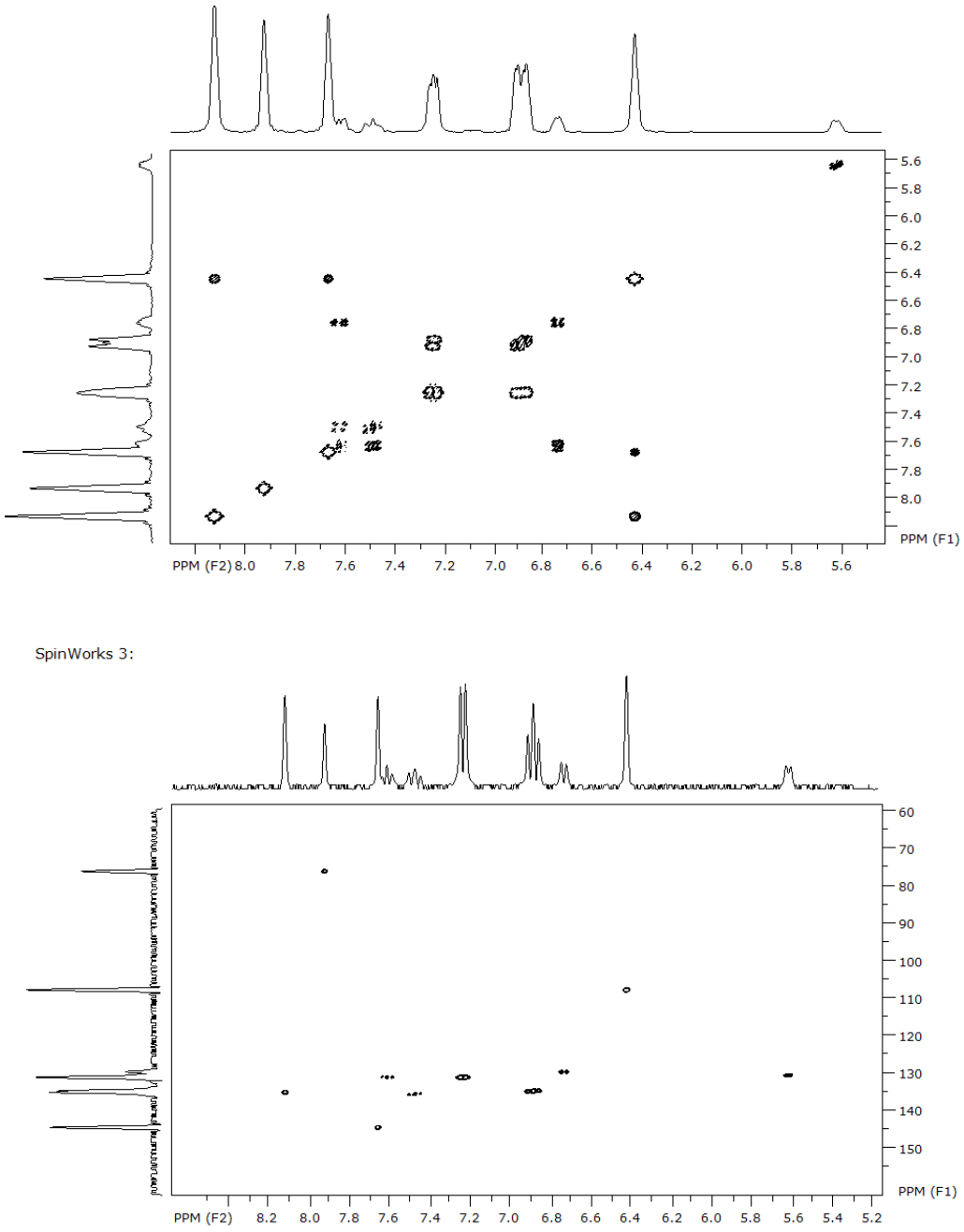

Figure S11. COSY (top) and HMQC (bottom) NMR spectrum of **2** in CD_3CN.

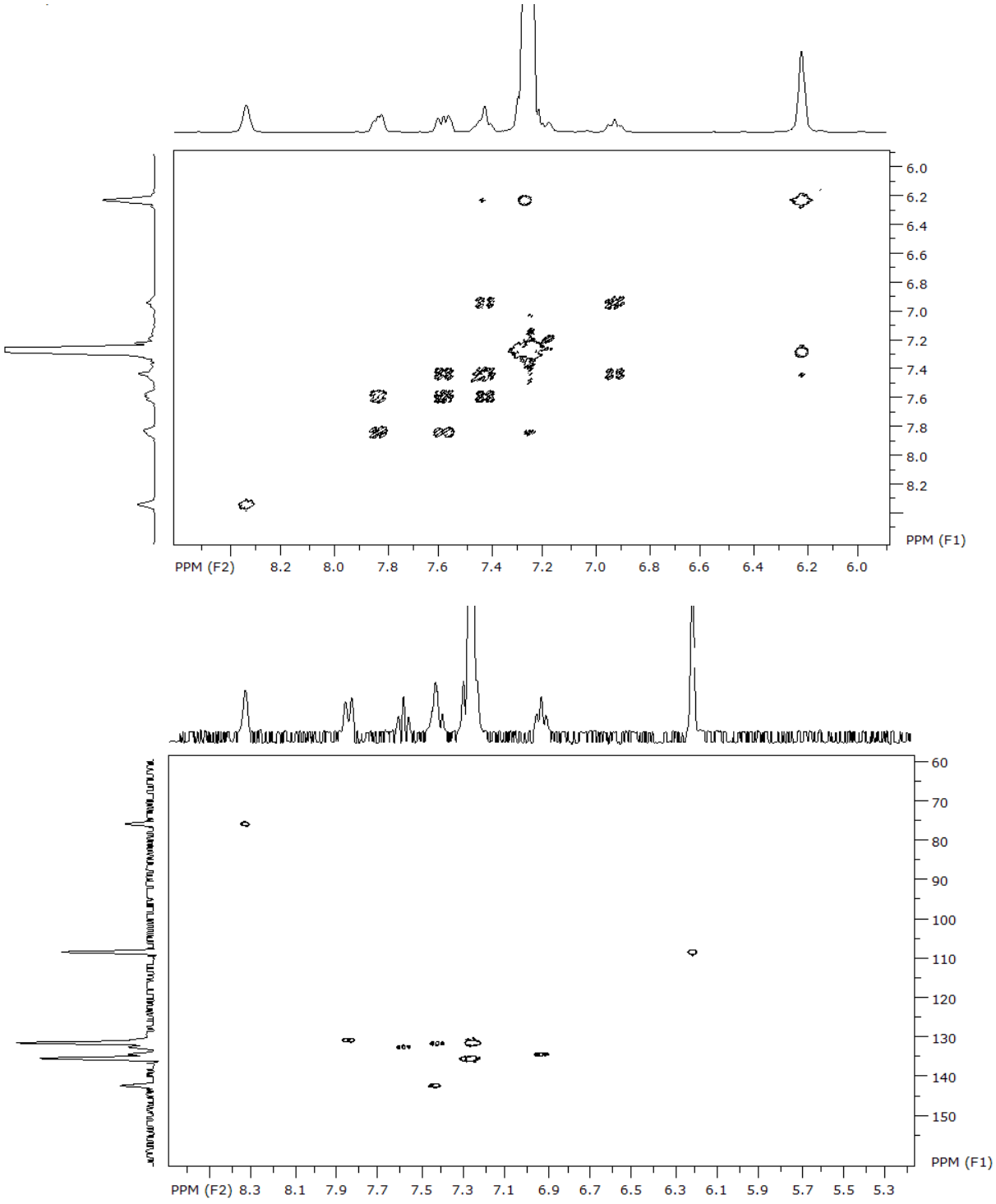

Figure S12. COSY (top) and HMQC (bottom) NMR spectrum of **3** in CD_3CN.

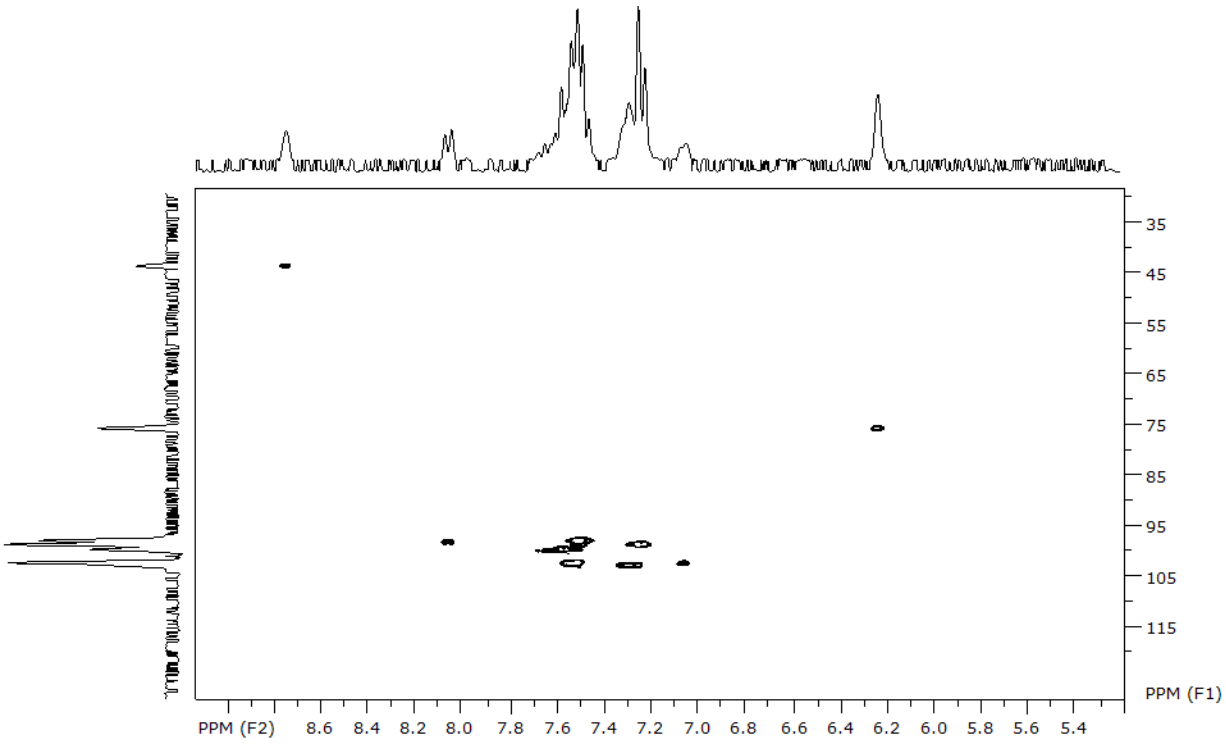

Figure S13. HMQC NMR spectrum of **4** in CD_3CN.

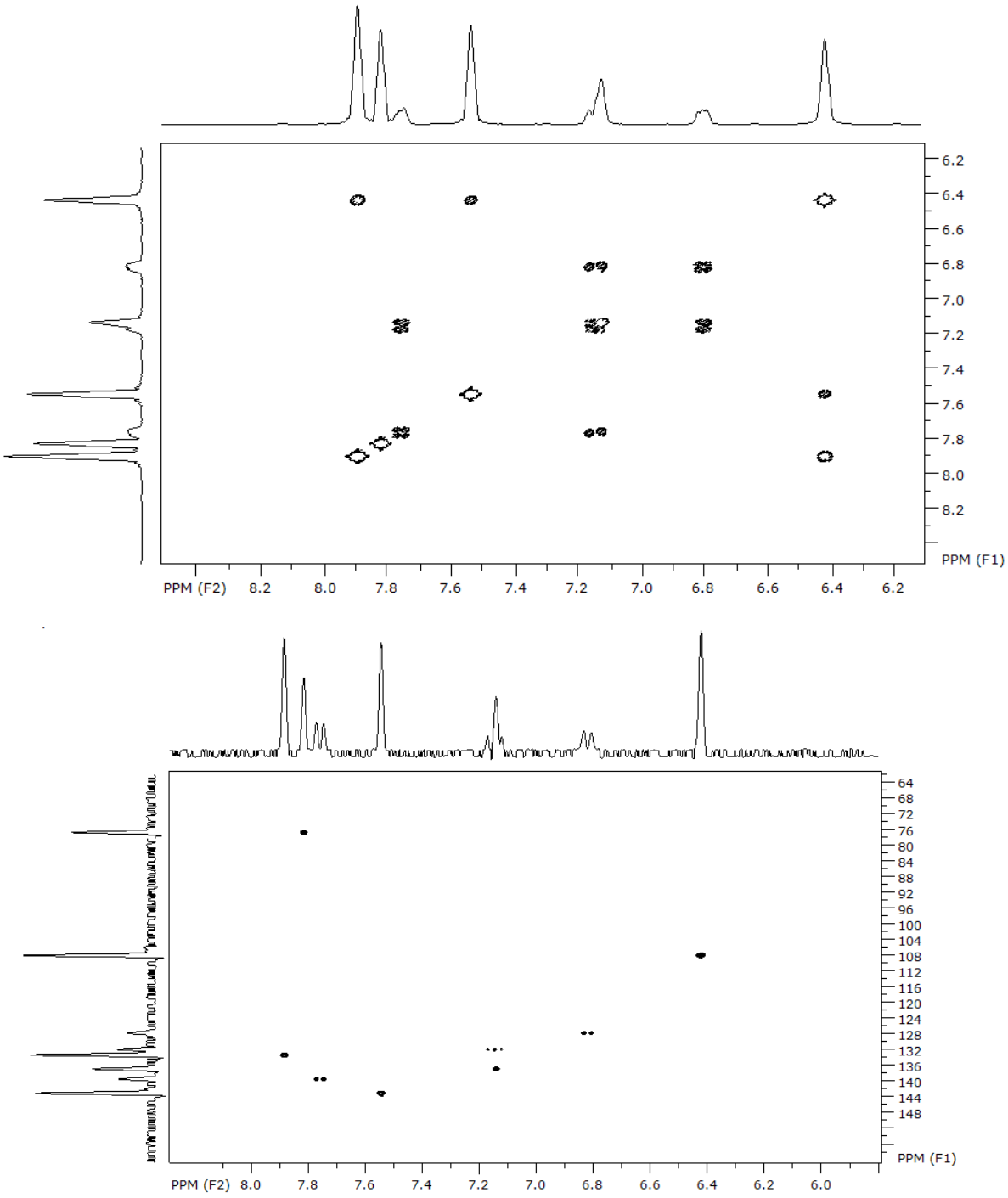

Figure S14. COSY (top) and HMQC (bottom) NMR spectrum of **5** in CD_3CN.

References.

(S1) CSD User Manuals; Cambridge Crystallographic Data Centre, 12 Union Road, Cambridge CB2 1EZ, U.K.

(S2) (a) Wheeler, S. E.; Bloom, J. W. G. *J. Phys. Chem. A* **2014,** Advance Article. (b) Bernstein, J. *Cryst. Growth Des.*, **2013**, *13*, 961-964. (c) Gu, Y.; Kar, T.; Scheiner, S. *J. Am. Chem. Soc.*, **1999**, *121*, 9411–9422. (d) Desiraju, G. J. *Acc. Chem. Res.*, **1996**, *29*, 441–449. (e) Steiner, T.; Saenger, F. *J. Am. Chem. Soc.*, **1992**, *114*, 10146-10154. (f) Desiraju, G. J. *Acc. Chem. Res.*, **1991**, 24, 290–296. (f) Taylor, R.; Kennard O. *J. Am. Chem. Soc.* **1982**, *104*, 5063–5070.

(S3) (a) Sammes, M. P.; Harlow, R. L.; Simonsen, S. H. *J. Chem. Soc., Perkin Trans. 2*, **1976**, *10*, 1126-30. (b) Wu, D. Y.; Ren, Y.; Wang, X.; Tian, A. M.; Wong, N. B.; Li, Wai-Kee *J. Molec. Struct. THEOCHEM* **1999**, *459*, 171-176. (c) Dhumal, N. R.; Gejji, S. P. *Chem. Phys. Lett.*, **2004**, *397*, 185-193.

(S4) (a) Takahashi, H.; Tsuboyama, S.; Umezawa, Y.; Honda, K.; Nishio, M. *Tetrahedron*, **2000**, *56*, 6185–6191. (b) Tsuzuki, S.; Honda, K.; Uchimaru, T.; Mikami, M.; Tanabe, K. *J. Am. Chem.Soc.*, **2000**, *122*, 11450–11458. (c) Nishio, M.; Hirota, M.; Umezawa, Y. *The CH-π interaction: evidence, nature, and consequences*, Wiley-VCH, Inc: New York, 1998. (d) Umezawa, Y.; Tsuboyama, S.; Honda, K.; Uzawa, J.; Nishio, M. *Bull. Chem. Soc. Jpn* **1998**, *71*, 1207-1213. (e) Braga, D.; Grepioni, F.; Tedesco, E. *Organometallics* **1998**, *17*, 2669-2672.

(S5) (a) Choudhury, A. R.; Row, T. N. G. *Cryst. Growth Des.*, **2004**, *4*, 47–52. (b) van den Berg, J. A.; Seddon, K. R., *Cryst. Growth Des.* **2003**, *3*, 643. (c) Brammer , L.; Bruton E. A.; Sherwood, P. *New J. Chem.* **1999**, *23*, 965-968. (d) Grepioni, F.; Cojazzi, G.; Draper, S. M.; Scully, N.; Braga, D. *Organometallics* **1998**, *17*, 296-307. (e) Thalladi , V. R.; Weiss , H. -C.; Bläser , D.; Boese , R.; Nangia, A.; Desiraju, G. R.; *J. Am. Chem. Soc.*, **1998**, *120*, 8702–8710.

(S6) (a) Salonen, L. M.; Ellermann, M.; and Diederich, F. *Angew. Chem. Int. Ed.* **2011**, *50*, 4808 – 4842. (b) Lee, E. C.; Kim, D.; Jurečka, P.; Tarakeshwar, P.; Hobza, P.; Kim, K. S.; *J. Phys. Chem. A* **2007**, *111*, 3446-3457. (c) Janiak, C. *J. Chem. Soc., Dalton Trans.* **2000**, 3885–3896. (d) McGaughey, G. B.; Gagné, M.; Rappé, A. K. *J. Biol. Chem.* **1998**, *273*, 15458-15463. (e) Hunter, C. A.; Sanders, J. K. M. *J. Am. Chem. Soc.* **1990**, *112*, 5525-5534